Article

Redox-Noninnocence of the S,S‘-Coordinated Ligands in Bis(benzene-1,2-dithiolato)iron Complexes

Kallol Ray, Eckhard Bill, Thomas Weyhermller, and Karl Wieghardt

J. Am. Chem. Soc., **2005**, 127 (15), 5641-5654• DOI: 10.1021/ja040237l • Publication Date (Web): 22 March 2005

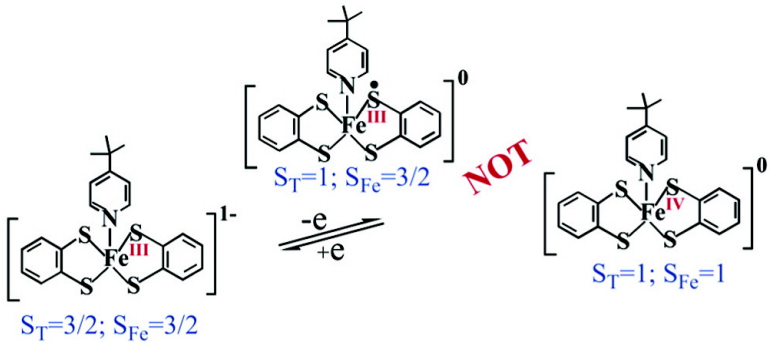

More About This Article

Additional resources and features associated with this article are available within the HTML version:

- Supporting Information
- Links to the 10 articles that cite this article, as of the time of this article download
- Access to high resolution figures
- Links to articles and content related to this article
- Copyright permission to reproduce figures and/or text from this article

View the Full Text HTML

J|A|C|S
ARTICLES
Published on Web 03/22/2005

Redox-Noninnocence of the S,S′-Coordinated Ligands in Bis(benzene-1,2-dithiolato)iron Complexes

Kallol Ray, Eckhard Bill, Thomas Weyhermüller, and Karl Wieghardt*

Contribution from the Max-Planck-Institute for Bioinorganic Chemistry, Stiftstrasse 34-36, D-45470 Mülheim an der Ruhr, Germany

Received October 14, 2004; E-mail: wieghardt@mpi-muelheim.mpg.de

Abstract: The electronic structures of complexes of iron containing two S,S′-coordinated benzene-1,2-dithiolate, $(L)^{2-}$, or 3,5-di-*tert*-butyl-1,2-benzenedithiolate, $(L^{Bu})^{2-}$, ligands have been elucidated in depth by electronic absorption, infrared, X-band EPR, and Mössbauer spectroscopies. It is conclusively shown that, in contrast to earlier reports, high-valent iron(IV) (d^4, $S = 1$) is not accessible in this chemistry. Instead, the S,S′-coordinated radical monoanions $(L^{\bullet})^{1-}$ and/or $(L^{Bu\bullet})^{1-}$ prevail. Thus, five-coordinate $[Fe(L)_2(PMe_3)]$ has an electronic structure which is best described as $[Fe^{III}(L)(L^{\bullet})(PMe_3)]$ where the observed triplet ground state of the molecule is attained via intramolecular, strong antiferromagnetic spin coupling between an intermediate spin ferric ion ($S_{Fe} = {}^3/_2$) and a ligand radical $(L^{\bullet})^{1-}$ ($S_{rad} = {}^1/_2$). The following complexes containing only benzene-1,2-dithiolate(2−) ligands have been synthesized, and their electronic structures have been studied in detail: $[NH(C_2H_5)_3]_2[Fe^{II}(L)_2]$ (**1**), $[N(n\text{-}Bu)_4]_2[Fe^{III}{}_2(L)_4]$ (**2**), $[N(n\text{-}Bu)_4]_2[Fe^{III}{}_2(L^{Bu})_4]$ (**3**); $[P(CH_3)Ph_3][Fe^{III}(L)_2(t\text{-}Bu\text{-}py)]$ (**4**) where *t*-Bu-py is 4-*tert*-butylpyridine. Complexes containing an $Fe^{III}(L^{\bullet})(L)$- or $Fe^{III}(L^{Bu})(L^{Bu\bullet})$- moiety are $[N(n\text{-}Bu)_4][Fe^{III}{}_2(L^{Bu})_3(L^{Bu\bullet})]$ (**3^{ox}**), $[Fe^{III}(L)(L^{\bullet})(t\text{-}Bu\text{-}py)]$ (**4^{ox}**), $[Fe^{III}(L^{Bu})(L^{Bu\bullet})(PMe_3)]$ (**7**), $[Fe^{III}(L^{Bu})(L^{Bu\bullet})(PMe_3)_2]$ (**8**), and $[Fe^{III}(L^{Bu})(L^{Bu\bullet})(PPr_3)]$ (**9**), where Pr represents the *n*-propyl substituent. Complexes **2**, **3^{ox}**, **4**, $[Fe^{III}(L)(L^{\bullet})(PMe_3)_2]$ (**6**), and **9** have been structurally characterized by X-ray crystallography.

Introduction

Coordination compounds of toluene-3,4-dithiolate, $(L^{Me})^{2-}$, with iron ions have been known since 1963 when Gray et al.[1−3] reported the synthesis of the dinuclear dianion $[Fe^{III}{}_2(L^{Me})_4]^{2-}$. The crystal structure of $[N(n\text{-}Bu)_4]_2[Fe_2(L^{Me})_4]$ was reported in 1986.[4] Later, the corresponding complex containing the unsubstituted benzene-1,2-dithiolate, $(L)^{2-}$, namely $[NEt_4]_2[Fe^{III}{}_2(L)_4]$, was synthesized and structurally characterized.[5,6] All early room-temperature crystal structure determinations have large standard deviations of the bond lengths which do not allow a detailed description of the electronic structure of the dianions. Recently, a better structure was reported for the 4,5-dicyanobenzene-1,2-dithiolato analogue $[Fe^{III}{}_2(L^{CN})_4][N(n\text{-}Bu)_4]_2$.[7] Although, all investigations agree that these dianions possess a diamagnetic ground state, contradicting proposals for the intrinsic spin of the ferric ions as $S_{Fe} = {}^3/_2$ (intermediate spin) or $S = {}^1/_2$ (low spin) have been reported.[8]

Interestingly, Holm et al.[8] have shown that the dianion $[Fe_2(L^{Me})_4]^{2-}$ can chemically be one-electron oxidized by iodine yielding $[N(n\text{-}Bu)_4][Fe_2(L^{Me})_4]$ which possesses an $S = {}^1/_2$ ground state. Its molecular and electronic structure has remained elusive. The question of metal (Fe^{III}/Fe^{IV}) or ligand ($(L^{Me})^{2-}/(L^{Me\bullet})^{1-}$) based mixed valency has not been addressed.

Monomeric, five-coordinate monoanions $[Fe^{III}(L)_2X]^{1-}$ where X represents a neutral ligand such as pyridine[2] or hydrazine[9] have been reported, and in both cases an $S = {}^3/_2$ ground state has been deduced from room-temperature magnetic susceptibility measurements. The structure of the former has not been reported.

Monomeric ferrous complexes $[Fe^{II}(L)_2]^{2-}$ and $[Fe^{II}(L)(PMe_3)_3]$ have been synthesized and structurally characterized.[10,11] We have recently shown[12] that square planar $[Fe^{II}(L)_2]^{2-}$ possesses an $S = 1$ ground state with a large zero-field splitting of $D = +28$ cm^{-1}. $[Fe^{II}(L)(PMe_3)_3]$ is five-coordinate and diamagnetic ($S = 0$), the iron ion is in a square-pyramidal S_2P_3 donor atom environment.

In 1991, Sellmann et al.[13] published an interesting paper where the "stabilization of high-valent Fe(IV) centers" in the

(1) Gray, H. B.; Billig, E. *J. Am. Chem. Soc.* **1963**, *85*, 2019.
(2) Williams, R.; Billig, E.; Waters, J. H.; Gray, H. B. *J. Am. Chem. Soc.* **1966**, *88*, 43.
(3) Baker-Hawkes, M.-J.; Billig, E.; Gray, H. B. *J. Am. Chem. Soc.* **1966**, *88*, 4870.
(4) Sawyer, D. T.; Srivatsa, G. S.; Bodini, M. E.; Schaefer, W. P.; Wing, R. M. *J. Am. Chem. Soc.* **1986**, *108*, 936.
(5) Wong, L.; Kang, B. *J. Struct. Chem.* **1987**, *6*, 94.
(6) Kang, B. S.; Weng, L. H.; Wu, D. X.; Wang, F.; Guo, Z.; Huang, L. R.; Huang, Z. Y.; Liu, H. Q. *Inorg. Chem.* **1988**, *27*, 1129.
(7) Alves, H.; Simao, D.; Novais, H.; Santos, I. C.; Gimenez-Saiz, C.; Gama, V.; Waerenborgh, J. C.; Henriques, R. T.; Almeida, M. *Polyhedron* **2003**, *22*, 2481.
(8) (a) Balch, A. L.; Holm, R. H. *Chem. Commun.* **1966**, 552. (b) Balch, A. L.; Dance, I. G.; Holm, R. H. *J. Am. Chem. Soc.* **1968**, *90*, 1139.
(9) Sellmann, D.; Kreutzer, P.; Huttner, G.; Frank, A. *Z. Naturforsch.* **1978**, *33b*, 1341.
(10) Sellmann, D.; Kleine-Kleffmann, U.; Zapf, L.; Huttner, G.; Zsolnai, L. *J. Organomet. Chem.* **1984**, *263*, 321.
(11) Sellmann, D.; Geck, M.; Moll, M. *J. Am. Chem. Soc.* **1991**, *113*, 5259.
(12) Ray, K.; Begum, A.; Weyhermüller, T.; van Slageren, J.; Neese, F.; Wieghardt, K. *J. Am. Chem. Soc.* **2005**, *127*, 4403.
(13) Sellmann, D.; Geck, M.; Knoch, F.; Ritter, G.; Dengler, J. *J. Am. Chem. Soc.* **1991**, *113*, 3819.

Scheme 1. Complexes

Complexes

$[Fe^{II}(L)_2]^{2-}$	**1**	ref. 10-12.
$[Fe^{III}_2(L)_4]^{2-}$	**2**	ref. 5,6.
$[Fe^{III}_2(L^{Bu})_4]^{2-}$	**3**	this work.
$[Fe^{III}_2(L^{Bu})_3(L^{Bu\bullet})]^{1-}$	$\mathbf{3^{ox}}$	this work
$[Fe^{III}(L)_2(^tBu\text{-}py)]^{1-}$	**4**	this work
$[Fe^{III}(L)(L^{\bullet})(^tBu\text{-}py)]^{0}$	$\mathbf{4^{ox}}$	this work
$[Fe^{III}(L)(L^{\bullet})(PMe_3)]^{0}$	**5**	ref. 13
$[Fe^{III}(L^{\bullet})_2(PMe_3)]^{+}$	$\mathbf{5^{ox}}$	ref. 13
$[Fe^{III}(L)(L^{\bullet})(PMe_3)_2]^{0}$	**6**	ref. 13
$[Fe^{III}(L)_2(PMe_3)_2]^{1-}$	$\mathbf{6^{red}}$	ref. 13
$[Fe^{III}(L^{Bu})(L^{Bu\bullet})(PMe_3)]^{0}$	**7**	this work
$[Fe^{III}(L^{Bu\bullet})_2(PMe_3)]^{+}$	$\mathbf{7^{ox}}$	this work
$[Fe^{III}(L^{Bu})(L^{Bu\bullet})(PMe_3)_2]^{0}$	**8**	this work
$[Fe^{III}(L^{Bu})_2(PMe_3)_2]^{1-}$	$\mathbf{8^{red}}$	this work
$[Fe^{III}(L^{Bu})(L^{Bu\bullet})(P^iPr_3)]^{0}$	**9**	this work

six-coordinate complex $[Fe^{IV}(L)_2(PMe_3)_2]$ and its five-coordinate analogue $[Fe^{IV}(L)_2(PMe_3)]$ was claimed. Both species were shown to possess an $S = 1$ ground state in agreement with a low-spin d^4 electron configuration of an Fe^{IV} ion. Zero-field Mössbauer data were also reported which apparently supported the above proposal. Both compounds are described as green-black crystalline materials with intense ($\sim 10^4$ M^{-1} cm^{-1}) absorption maxima in the near-infrared (>600 nm). We felt that this observation is not in accord with the proposed electronic structure as Fe(IV) species.

We have recently shown[14,15] that S,S′-coordinated benzene-1,2-dithiolato(2−) ligands are readily oxidized by one electron yielding an S,S′-coordinated benzene-1,2-dithiolato(1−) π radical anion, $(L^{\bullet})^{1-}$.[14,15] In this case, the electronic structure of the above complexes would have to be reformulated as $[Fe^{III}(L)(L^{\bullet})(PMe_3)_2]$ and $[Fe^{III}(L)(L^{\bullet})(PMe_3)]$ where the $S = 1$ ground state would result from a very strong intramolecular antiferromagnetic coupling between an intermediate spin ferric ion ($S_{Fe} = {}^3/_2$) and a ligand π radical ($S_{rad} = {}^1/_2$). We note that Sawyer et al.[4] have suggested that in $[N(n\text{-}Bu)_4]_2[Fe_2(L^{Me})_4]$ the iron ions may possess an +II oxidation state with $S = 2$. In this case, one antiferromagnetically coupled π radical anion per $[Fe^{II}(L^{Me})(L^{Me\bullet})]^{1-}$ unit must exist. No spectroscopic evidence for this notion was given.

In view of these contradicting interpretations we have initiated the following, in depth, synthetic and spectroscopic study. We have synthesized and studied spectroscopically the complexes shown in Scheme 1 by using the ligands shown in Scheme 2.

Experimental Section

Synthesis of Complexes. $[NH(C_2H_5)_3]_2[Fe^{II}(L)_2]$ (**1**),[12] $[Fe(L)_2(PMe_3)]$ (**5**),[13] and $[Fe(L)_2(PMe_3)_2]$ (**6**)[13] have been prepared according

Scheme 2

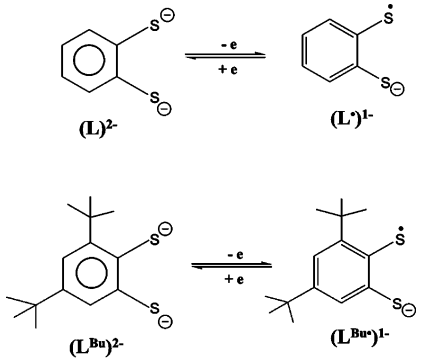

to procedures described in the literature. The ligand 3,5-di-*tert*-butyl-1,2-benzenedithiol, $H_2[L^{Bu}]$, has been synthesized as described in ref 16.

$[N(n\text{-}Bu)_4]_2[Fe_2(L)_4]$ (2). To a solution of 1,2-benzenedithiol, $H_2[L]$ (0.28 g; 2.0 mmol), in dry, degassed methanol (40 mL) were added under strictly anaerobic conditions (Ar blanketing atmosphere) triethylamine (0.4 mL; 4.0 mmol) and $FeCl_2 \cdot 4H_2O$ (0.20 g; 1.0 mmol) and $[N(n\text{-}Bu)_4](PF_6)$ (0.78 g; 2.0 mmol). After being stirred at ambient temperature for 15 min the solution was allowed to stand for 12 h at 20 °C during which time light yellow crystals of $[N(n\text{-}Bu)_4][Fe^{II}(L)_2]$ (**1**) precipitated and were collected by filtration and redissolved in an acetone/toluene mixture (1:1 vol). Slow evaporation of the solvent in the presence of air produced black cubes of **2** suitable for X-ray crystallography. Yield: 0.15 g.

$[N(n\text{-}Bu)_4]_2[Fe_2(L^{Bu})_4]$ (3). Sodium metal (0.069 g; 3.0 mmol) was added to a solution of $[N(n\text{-}Bu)_4]Br$ (0.161 g; 0.5 mmol) and $H_2[L^{Bu}]$ (0.25 g; 1.0 mmol) in absolute ethanol (10 mL) under an argon blanketing atmosphere. A solution of $FeCl_3$ (0.081 g; 0.5 mmol) in degassed ethanol (5 mL) was slowly added to the above solution at 20 °C under anaerobic conditions in the glovebox. The resultant dark red solution was stirred for 30 min during which time dark black microcrystalline **3** precipitated. Yield: 224 mg (56%). Anal. Calcd for $C_{88}H_{152}S_8Fe_2N_2$: C, 65.80; H, 9.54; N, 1.74. Found: C, 65.7; H, 9.3; N, 1.8. Electrospray mass spectrum (CH_2Cl_2 solution) positive- and negative-ion mode: $m/z = 560$ $\{Fe(L^{Bu})_2\}^-$; 242 $\{N(n\text{-}Bu)_4\}^+$.

$[N(n\text{-}Bu)_4][Fe_2(L^{Bu})_4]$ ($\mathbf{3^{ox}}$). Sodium metal (0.069 g; 3.0 mmol) was added to a solution of $H_2[L^{Bu}]$ (0.25 g; 1.0 mmol) in absolute ethanol (10 mL) under an argon blanketing atmosphere. Solid $FeCl_3$ (0.081 g; 0.5 mmol) was added to this solution. The resultant dark red solution was exposed to air and stirred for 5 min. The solution was then filtered, and to the filtrate was added a solution of $[N(n\text{-}Bu)_4]Br$ (0.161 g; 0.5 mmol) in ethanol (5 mL). Microcrystalline greenish black $\mathbf{3^{ox}}$ precipitated from the solution. Yield: 136 mg (40%). Anal. Calcd for $C_{72}H_{116}S_8Fe_2N$: C, 63.44; H, 8.52; N, 1.03. Found: C, 64.49; H, 8.20; N, 1.20. Electrospray mass spectrum (CH_2Cl_2 solution) positive- and negative-ion mode: $m/z = 560$ $\{Fe(L^{Bu})_2\}^-$; 242 $\{N(n\text{-}Bu)_4\}^+$.

$[P(CH_3)Ph_3][Fe(L)_2(t\text{-}Bu\text{-}py)]$ (4). Sodium metal (0.069 g; 3.0 mmol) was added to a solution of $H_2[L]$ (0.14 g; 1.0 mmol) and 4-*tert*-butylpyridine (2 mL) in absolute ethanol (10 mL) under an argon blanketing atmosphere. Solid $FeCl_3$ (0.081 g; 0.5 mmol) was added to this solution. A dark red powder of **4** precipitated upon addition of $[P(CH_3)Ph_3]Br$ (0.180 g; 0.5 mmol) to the resultant dark red solution. Yield: 300 mg (80%). Anal. Calcd for $C_{40}H_{39}S_4FeNP$: C, 64.16; H, 5.25; N, 1.87. Found: C, 64.19; H, 5.40; N, 1.91. Electrospray mass spectrum (CH_2Cl_2 solution with a few drops of 4-*tert*-butylpyridine) positive- and negative-ion mode: $m/z = 471.6$ $\{Fe(L)_2(4\text{-}^tBuPy)\}^-$; 277.3 $\{P(Me)Ph_3\}^+$. Single crystals suitable for X-ray crystallography

(14) Ghosh, P.; Begum, A.; Herebian, D.; Bothe, E.; Hildenbrand, K.; Weyhermüller, T.; Wieghardt, K. *Angew. Chem., Int. Ed.* **2003**, *42*, 563.
(15) Ray, K.; Weyhermüller, T.; Goossens, A.; Crajé, M. W. J.; Wieghardt, K. *Inorg. Chem.* **2003**, *42*, 4082.
(16) (a) Sellmann, D.; Freyberger, G.; Eberlein, R.; Böhlen, E.; Huttner, G.; Zsolnai, L. *J. Organomet. Chem.* **1987**, *323*, 21. (b) Sellmann, D.; Käppler, O. *Z. Naturforsch.* **1987**, *42b*, 1291.

Table 1. Crystallographic Data for **2**, **3^{ox}**, **4**, **6**, and **9**

	2	**3^{ox}**	**4**	**6**	**9**
chem formula	$C_{56}H_{88}Fe_2N_2S_8$	$C_{72}H_{116}Fe_2NS_8$	$C_{40}H_{39}FeNPS_4$	$C_{18}H_{26}FeP_2S_4$	$C_{37}H_{61}FePS_4$
fw	1157.46	1363.84	748.78	488.42	720.92
space grp	*P*-1, *No. 2*	*P*-1, *No. 2*	*Cc*, No. 9	$P2_12_12$, No. 18	*Pnma*, No. 62
a, Å	12.6561(6)	14.018(2)	12.3310(3)	11.9489(4)	53.472(4)
b, Å	15.0960(8)	17.260(3)	24.7174(5)	20.6634(8)	7.0995(8)
c, Å	16.1084(8)	18.196(4)	12.3106(4)	8.6716(4)	10.6898(12)
α, deg	85.12(1)	73.91(2)	90	90	90
β, deg	88.24(1)	69.65(2)	99.19(1)	90	90
γ, deg	75.24(1)	82.85(2)	90	90	90
V, Å^3	2965.1(3)	3964.1(12)	3704.0(2)	2141.1(2)	4058.1(7)
Z	2	2	4	4	4
T, K	100(2)	100(2)	100(2)	100(2)	100(2)
ρ calcd, g cm^{-3}	1.296	1.143	1.343	1.515	1.180
refl. collected/2Θ$_{max}$	35992/66.4	8632/42.0	53762/62.0	46345/61.1	19492/47.0
unique reflns/$I > 2\sigma(I)$	22272/15817	6656/4033	11737/11069	6549/6439	3181/2307
no. of params/restr	613/0	748/1	428/2	232/0	256/0
μ(Mo Kα), cm^{-1}	8.08	6.13	7.05	12.44	12.88
R1[a]/ goodness of fit [b]	0.0509/1.017	0.0956/1.107	0.0293/1.037	0.0172/1.046	0.0893/1.196
wR2 [c]($I > 2\sigma(I)$)	0.0931	0.1601	0.0599	0.0432	0.1494
resid density, e Å^{-3}	+0.53/−0.71	+0.40/−0.36	+0.28/−0.28	+0.42/−0.32	+0.74/−0.46

[a] Observation criterion: $I > 2\sigma(I)$. $R1 = \Sigma||F_o| - |F_c||/\Sigma|F_o|$. [b] $GoF = [\Sigma[w(F_o^2 - F_c^2)^2]/(n-p)]^{1/2}$. [c] $wR2 = [\Sigma[w(F_o^2 - F_c^2)^2]/\Sigma[w(F_o^2)^2]]^{1/2}$ where $w = 1/\sigma^2(F_o^2) + (aP)^2 + bP$, $P = (F_o^2 + 2F_c^2)/3$.

were obtained by recrystallization of this material from a CH_2Cl_2/toluene mixture (1:1 by volume).

[Fe(L)$_2$(*t*-Bu-py)] (4^{ox}). To a solution of **4** (0.05 g; 0.07 mmol) in CH_3CN was added a few drops of 4-*tert*-butylpyridine. The resultant solution was cooled to −30 °C, and solid tris(4-bromophenyl)amminium hexachloroantimonate (0.06 g; 0.07 mmol) was added. The solution was then frozen to liquid nitrogen temperature and used for Mössbauer measurements.

[Fe(L^{Bu})$_2$(PMe$_3$)] (7). A gentle stream of N_2 was bubbled through the boiling blue-green toluene solution (30 mL) of **8** (0.20 g; 0.28 mmol) for 1 h. The solution was filtered while hot, whereupon microcrystalline **7** crystallizes out from solution. Yield: 106 mg (60%). Anal. Calcd for $C_{31}H_{49}S_4FeP$: C, 58.47; H, 7.76. Found: C, 58.31; H, 7.90. Electrospray mass spectrum (CH_2Cl_2 solution) positive ion mode: $m/z = 636$ {Fe(L^{Bu})$_2$(PMe$_3$)}$^+$.

[Fe(L^{Bu})$_2$(PMe$_3$)](SbCl$_6$) (7^{ox}). To a CH_2Cl_2 solution (10 mL) of **7** (0.03 g; 0.05 mmol) at −30 °C was added 1 equiv of tris(4-bromophenyl)aminium hexachloroantimonate (0.04 g; 0.05 mmol). The solvent was removed at −30 °C by rotary evaporation. The blackish residue of **7^{ox}** was cooled to liquid nitrogen temperature and used for Mössbauer measurements. Complex **7^{ox}** proved to be very unstable at room temperature, and further characterizations have not been possible to date.

[Fe(L^{Bu})$_2$(PMe$_3$)$_2$] (8). A solution of NaOMe (0.107 g; 2 mmol) and H$_2$[L^{Bu}] (0.25 g; 1.0 mmol) in 10 mL of methanol was combined with a solution of $FeCl_3$ (0.081 g; 0.5 mmol) in 3 mL of methanol under an argon blanketing atmosphere. Addition of PMe_3 (0.2 mL, 2 mmol) and filtration afforded a red-violet solution. Bubbling oxygen through this solution for 2 min yielded a dark green suspension. The black-green microcrystals of **8** were collected by filtration, washed with methanol, and dried. Yield: 292 mg (82%). Anal. Calcd for $C_{34}H_{58}S_4FeP_2$: C, 57.29; H, 8.20. Found: C, 57.34; H, 8.06. Electrospray mass spectrum (CH_2Cl_2 solution) positive ion mode: $m/z = 636$ {Fe(L^{Bu})$_2$(PMe$_3$)}$^+$.

[Fe(L^{Bu})$_2$(PPr$_3$)] (9). A solution of NaOMe (0.107 g; 2 mmol) and H$_2$[L^{Bu}] (0.25 g; 1.0 mmol) in 10 mL of methanol was combined with a solution of $FeCl_3$ (0.081 g; 0.5 mmol) in 3 mL of methanol under argon blanketing conditions. Addition of tris(*n*-propyl)phosphane (0.5 mL, 2 mmol) and filtration gave a red-violet solution. Bubbling oxygen through this solution for 2 min yielded a dark green suspension. The crude crystalline product obtained by filtration is recrystallized from a 1:1 mixture (volume) of CH_2Cl_2 and toluene to yield deep black rectangular crystals of **9**. Yield: 200 mg (56%). Anal. Calcd for $C_{37}H_{61}S_4FeP$: C, 61.64; H, 8.53. Found: C, 61.57; H, 8.32. Electrospray mass spectrum (CH_2Cl_2 solution) positive-ion mode: $m/z = 720$ {Fe(L^{Bu})$_2$(P(Pr)$_3$)}$^+$.

Physical Measurements. The equipment used for IR, UV−vis−NIR, X-band EPR, and Mössbauer spectroscopies has been described in ref 15. The temperature-dependent magnetic susceptibilities of solid samples of complexes were measured by using a SQUID magnetometer (Quantum Design) at 1.0 T (2.0−300 K). Corrections for underlying diamagnetism were made by using tabulated Pascal's constants. Cyclic voltammograms and coulometric experiments were performed with an EG&G potentiostat/galvanostat in CH_2Cl_2 solutions (0.10 M [N(*n*-Bu)$_4$]-PF_6) at a glassy carbon working electrode. Ferrocene was used as internal standard; all redox potentials are given vs the ferrocenium/ferrocene (Fc^+/Fc) couple.

X-ray Crystallographic Data Collection and Refinement of the Structures. Dark red single crystals of **4** and **9** and black crystals of **2**, **3^{ox}**, and **6** were coated with perfluoropolyether, picked up with a glass fiber, and mounted in the nitrogen cold stream of the diffractometer. Intensity data were collected at 100 K using a Nonius Kappa-CCD diffractometer equipped with a Mo-target rotating-anode X-ray source and a graphite monochromator (Mo Kα, $\lambda = 0.71073$ Å). Final cell constants were obtained from a least-squares fit of all measured reflections. Crystal faces, except for compound **2**, were determined and the corresponding intensity data were corrected for absorption using the Gaussian-type routine embedded in XPREP.[17] The data set of **2** was left uncorrected. Crystallographic data of the compounds are listed in Table 1. The Siemens ShelXTL[17] software package was used for solution and artwork of the structure, ShelXL97[18] was used for the refinement. The structures were readily solved by direct and Patterson methods and subsequent difference Fourier techniques. All non-hydrogen atoms were refined anisotropically and hydrogen atoms were placed at calculated positions and refined as riding atoms with isotropic displacement parameters.

Complex **9** was first solved and refined in the acentric space group *Pna*2$_1$ (No.33) but the crystal appeared to be twinned by merohedry giving rise to apparent disorder, mainly of the iron and the phosphorus atom splitting on two positions. The structure was therefore finally refined in centrosymmetric space group *Pnma* (No.62), now having a mirror plane running through the basal S_4-plane which "generates the former split positions" (the iron center is off plane). The occupation

(17) *ShelXTL V.5*; Siemens Analytical X-ray Instruments, Inc.: Madison, WI, 1994.
(18) Sheldrick, G. M. *ShelXL97*; Universität Göttingen: Göttingen, Germany, 1997.

factor of the phosphane ligand (above and below the pseudoplane) was set to 0.5 to account for the "disorder".

Results

Syntheses and Characterization of Complexes. As has been established by Sellmann and co-workers,[10,11] the reaction of dilithium benzene-1,2-dithiolate(2−) with $FeCl_2 \cdot 4H_2O$ (2:1) under strictly anaerobic conditions in tetrahydrofuran yields upon addition of $[AsPh_4]Cl$, $[NH(C_2H_5)_3]Br$, or $[N(n\text{-}Bu)_4]Br$ the yellow crystalline salts $[monocation]_2[Fe^{II}(L)_2]$ (**1**). The square-planar dianion possesses an $S = 1$ ground state and a large positive[12] zero-field splitting parameter, D, of $+28$ cm^{-1}. The molecular structure[10,12] clearly shows the presence of two closed-shell benzene-1,2-dithiolate dianions. The average C−S bond lengths at 1.76 ± 0.01 Å are typical for S,S′-coordinated benzene-1,2-dithiolates, and the C−C distances of two six-membered, aromatic phenyl rings are equidistant at 1.398 ± 0.006 Å as expected. The electronic structure has been verified by density functional theoretical calculations[12] which clearly show the presence of an intermediate spin ferrous ion ($S = 1$). Thus, the Mössbauer parameters of the $[Fe^{II}(L)_2]^{2-}$ ion[11] are considered to be a benchmark for such a square planar $Fe^{II}S_4$ core.

Oxidation of **1** in poorly coordinating solvents produces the dimeric species $[monocation]_2[Fe^{III}_2(L)_4]$ (**2**) (monocation = $[N(C_2H_5)_4]^+$, $[N(n\text{-}Bu)_4]^+$).[5,6] From a structural reinvestigation of $[N(n\text{-}Bu)_4]_2[Fe^{III}_2(L)_4]$ in this work (see below) it is established that the ligands are S,S′-coordinated, closed-shell dianions $(L)^{2-}$ with the central iron ions being ferric. Thus, the oxidation of **1** to **2** is metal centered and accompanied by dimerization. The crystal structure of **2** does not support the notion that **2** may possess an electronic structure such as $[Fe^{II}_2(L^{\bullet})_2(L)_2]^{2-}$ as has been suggested by Sawyer et al.[4]

By using disodium 3,5-di-*tert*-butyl-1,2-benzenedithiolate, $Na_2[L^{Bu}]$, as a ligand it has been possible to isolate the analogous crystalline black salt $[N(n\text{-}Bu)_4]_2[Fe^{III}_2(L^{Bu})_4]$ (**3**). The reaction of $Na_2[L^{Bu}]$ with $Fe^{III}Cl_3$ (2:1) in ethanol under anaerobic conditions also yields **3** upon addition of $[N(n\text{-}Bu)_4]Br$. Interestingly, the reaction of **3** dissolved in a CH_2Cl_2/CH_3OH mixture (1:1 vol) with a small amount of dioxygen yielded greenish-black crystals of $[N(n\text{-}Bu)_4][Fe_2(L^{Bu})_4]$ (**3^{ox}**) suitable for X-ray crystallography. It contains the dinuclear monoanion $[Fe_2(L^{Bu})_4]^-$. Thus, the dianion $[Fe^{III}_2(L^{Bu})_4]^{2-}$ in **3** is oxidized by one electron. A metal-centered oxidation of **3** would yield a mixed valent species $Fe^{III}Fe^{IV}$ but, of course, ligand oxidation must also be considered to be a viable alternative affording $[Fe^{III}_2(L^{Bu})_3(L^{Bu\bullet})]^-$. As we will show below the latter is the case for **3^{ox}** which is the analogue of Holm's complex $[N(n\text{-}Bu)_4][Fe_2(L^{Me})_4]$.[8]

The dimer $[Fe^{III}_2(L)_4]^{2-}$ is known[2,3] to react in coordinating solvents such as pyridine with formation of the square-base pyramidal monomer $[Fe^{III}(L)_2(py)]^-$ which possesses an intermediate spin ground state ($S = {}^3/_2$).[3,7] This species has not been structurally characterized to date. Therefore, we have prepared and isolated $[P(CH_3)Ph_3][Fe^{III}(L)_2(t\text{-Bu-py})]$ (**4**) and characterized it by X-ray crystallography (*t*-Bu-py is 4-*tert*-butylpyridine). The presence of two closed-shell dianions $(L)^{2-}$ is clearly seen which renders the iron ion ferric ($S_{Fe} = {}^3/_2$).

It is interesting that the axial ligand in **4** can be substituted by a phosphine such as trimethylphosphine yielding the anion $[Fe(L)_2(PMe_3)]^-$ which has not been isolated to date. This putative anion is readily oxidized in the presence of dioxygen yielding neutral, five-coordinate $[Fe(L)_2(PMe_3)]$ (**5**). The oxidation has been proposed to be metal-centered yielding an $[Fe^{IV}(L)_2(PMe_3)]$ species.[13] Similarly, the reaction of $Na_2[L]$ with $FeCl_3$ and PMe_3 (2:1:2) in methanol yields six-coordinate, black $[NMe_4][Fe^{III}(L)_2(PMe_3)_2]$ with a doublet ground state ($S = {}^1/_2$).[13] Its one-electron oxidation with dioxygen yields the neutral, six-coordinate species $[Fe(L)_2(PMe_3)_2]$ (**6**)[13] with a triplet ground state ($S = 1$). Complex **6** has also been described[13] as high valent iron(IV) species $[Fe^{IV}(L)_2(PMe_3)_2]$, whereas the corresponding monoanion ($S = {}^1/_2$) has been (correctly) assigned a ferric oxidation state as in $[Fe^{III}(L)_2(PMe_3)_2]^-$ the $[N(CH_3)_4]^+$ salt of which has been structurally characterized.[13]

To gain more insight into the electronic structures of these putative high valent complexes **5** and **6** we have synthesized the corresponding analogues $[Fe(L^{Bu})_2(PMe_3)]$ (**7**) and $[Fe(L^{Bu})_2(PMe_3)_2]$ (**8**) and $[Fe(L^{Bu})_2(PPr_3)]$ (**9**) where Pr is the *n*-propyl substituent. To systematically decrease the errors of the crystallographically determined bond lengths in **6** (at 298 K) we have reinvestigated the structure at 100 K (see below).

Table 2. Redox Potentials of Complexes[a] (V) vs Fc^+/Fc (CH_2Cl_2; 0.10 M $[N(n\text{-}Bu)_4]PF_6$)

complex	E^1, V	E^2, V	E^3, V	E^4, V
2	−1.36 (r; 2e)	−0.41 (r; 1e)	−0.10 (r; 1e)	
3	−1.45 (r; 2e)	−0.63 (r; 1e)	−0.35 (r; 1e)	+0.40 (qr; 1e)
4	−0.175 (r; 1e)			
5[b]	−1.42 (r; 1e)	−0.68 (r; 1e)	+0.28 (qr; 1e)	
6[b]	−1.45 (r; 1e)	−0.68 (r; 1e)	+0.30 (qr; 1e)	−0.10 (irr $E_{p,ox}$)
7	−1.50 (r; 1e)	−0.84 (r; 1e)	0.085 (r; 1e)	
8	−1.50 (r; 1e)	−0.83 (r; 1e)	0.085 (r; 1e)	−0.13 (irr $E_{p,ox}$)
9	−1.42 (r; 1e)	−0.79 (r; 1e)	0.17 (r; 1e)	

[a] r = reversible; qr = quasireversible; irr = irreversible. [b] Reference 13; the redox potentials have been converted from NHE to the Fc^+/Fc couple by addition of −0.4 V.

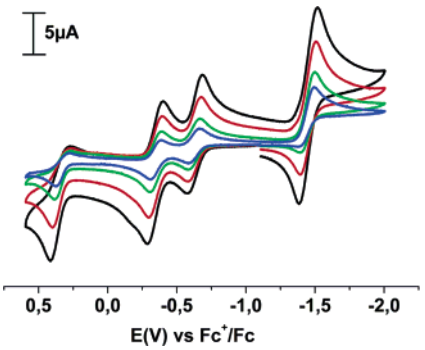

Figure 1. CV of **3** in CH_2Cl_2 solution (80.10 M $[N(n\text{-}Bu)_4]PF_6$) at 20 °C at a glassy carbon working electrode at scan rates 50, 100, 200, and 400 mV s^{-1}.

Electro- and Spectroelectrochemistry. Cyclic voltammograms (CVs) of **2**−**4**, **7**, and **8** have been recorded in CH_2Cl_2 solutions containing 0.10 M $[N(n\text{-}Bu)_4]PF_6$ as supporting electrolyte by a glassy carbon working electrode and a $Ag/AgNO_3$ reference electrode. Ferrocene was used as internal standard, and all potentials are referenced versus the ferrocenium/ferrocene couple (Fc^+/Fc). The results are summarized in Table 2.

Figure 1 shows the CV of **3** which displays one quasireversible and three reversible waves; the CV of **3^{ox}** is identical. Coulometric experiments at appropriately fixed potentials show

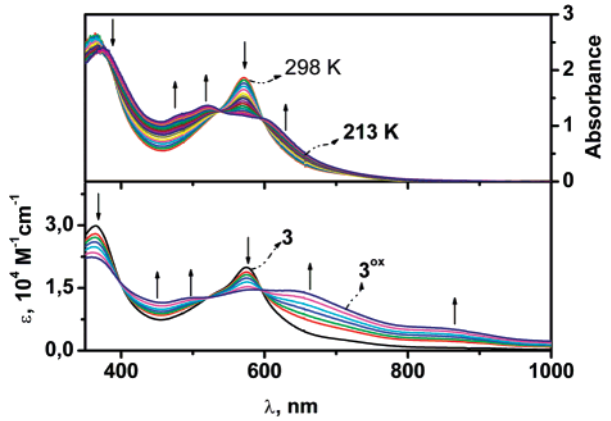

Figure 2. Electronic spectra of **3** in CH_2Cl_2 as a function of the temperature (range +25 to −60 °C) (top) and spectral changes associated with the coulometric one-electron oxidation of **3** to $\mathbf{3^{ox}}$ in CH_2Cl_2 at −25 °C (0.10 M $[N(n\text{-}Bu)_4]PF_6$).

that the first reversible wave at $E^1_{1/2} = -1.45$ V corresponds to a two-electron reduction of dinuclear **3** which may indicate two successive one-electron-transfer steps as in eq 1 yielding mononuclear $[Fe^{II}(L^{Bu})_2]^{2-}$.

$$[Fe_2{}^{III}L_4{}^{Bu}]^{2-} \underset{-2e}{\overset{+2e}{\rightleftharpoons}} 2[Fe^{II}L_2{}^{Bu}]^{2-} E^1{}_{1/2} \qquad (1)$$

The two waves at $E^2_{1/2} = -0.63$ V and $E^3_{1/2} = -0.35$ V each correspond to a one-electron oxidation per dimeric dianion in **3** as shown in eq 2.

$$[Fe_2{}^{III}L_4{}^{Bu}]^{2-} \underset{+1e}{\overset{-1e}{\rightleftharpoons}} [Fe_2L_4{}^{Bu}]^{1-} \underset{+1e}{\overset{-1e}{\rightleftharpoons}} [Fe_2L_4{}^{Bu}]^{0} \qquad (2)$$

Thus, one-electron oxidation of **3** yields reversibly the monoanion $\mathbf{3^{ox}}$ which can again be reversibly oxidized yielding a dinuclear neutral species. At this point it is not possible to discern between metal- or ligand-centered processes but from the following spectroscopic characterizations it is clear that the monoanion is $[Fe^{III}{}_2(L^{Bu})_3(L^{Bu\bullet})]^-$ which may indicate that the neutral species is $[Fe^{III}{}_2(L^{Bu})_2(L^{Bu\bullet})_2]^0$. The quasireversible one-electron-transfer process at $E^4_{1/2} = +0.40$ V has not been investigated in detail because the generated cationic species is not stable. The CV of **2** is very similar (Table 2) and the results are to be interpreted analogously.

Figure 2 displays the electronic spectra of **3** in CH_2Cl_2 solution as a function of the temperature (25° to −60 °C). Interestingly, there is a significant, reversible change of the electronic spectrum in this temperature range. This has been reported previously[19] for the dimer $[Co^{II}{}_2(L_S{}^{ISQ})_4]$ where $(L_S{}^{ISQ})^{1-}$ represents the π radical monoanion of 6-amino-2,4-di-*tert*-butylthiophenolate(2-). In analogy to this species the effect may be interpreted as valence tautomerism eq 3.

$$\underset{>298\ K}{[Fe_2{}^{III}L_4{}^{Bu}]^{2-}} \overset{K}{\rightleftharpoons} \underset{<213\ K}{[Fe_2{}^{II}(L^{Bu})_2(L^{Bu\bullet})_2]^{2-}} \qquad (3)$$

The spectrum of **3** at 298 K in CH_2Cl_2 solution resembles that of **4** (see below) which also displays a single intense LMCT transition at ~500 nm, whereas the spectrum at 213 K resembles that of $\mathbf{3^{ox}}$ or $\mathbf{4^{ox}}$ all three of which exhibit IVCT bands >600 nm. We have analyzed the spectral changes in Figure 2 on the assumption of the equilibrium shown in eq 3 and calculated the following thermodynamic data: $\Delta G^{300} = -2.2$ kJ mol^{-1}; $\Delta H = +11 \pm 1$ kJ mol^{-1}; $\Delta S^{300} = 44 \pm 3$ J mol^{-1} K^{-1}. Similar values have been reported by Pierpont et al.[20,21] for (catecholato)cobalt(III) ⇌ (semiquinonato)cobalt(II) equilibria and in ref 19 for the dinuclear $[Co^{III}(L_S{}^{IP})(L_S{}^{ISQ})]_2$. It is noted that this valence tautomeric equilibrium of **3** is only observed in solution. In the solid state, the spectrum of **3** does not change in the range 10−300 K. The solution spectrum of **2** also does not show this temperature dependence.

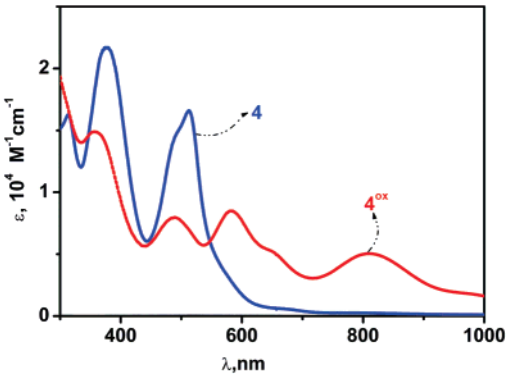

Figure 3. Electronic spectra of **4** and $\mathbf{4^{ox}}$ in CH_2Cl_2 solution at 20 °C.

Figure 2 (bottom) shows the spectral changes observed during the electrochemical oxidation of **3** to $\mathbf{3^{ox}}$ in CH_2Cl_2 solution (0.10 M $[N(n\text{-}Bu)_4PF_6$) at −25 °C. The appearance of intense absorption bands >600 nm is a clear indication for the presence of one S,S′-coordinated $(L^{Bu})^{2-}$ ligand and one $(L^{Bu\bullet})^{1-}$ radical in $\mathbf{3^{ox}}$.

The CV of mononuclear **4** (not shown) displays a fully reversible one-electron-transfer wave in CH_2Cl_2 solution (0.10 M $[N(n\text{-}Bu)_4]PF_6$) at 20 °C at $E^1_{1/2} = -0.175$ V in the potential range 0.0 to −0.8 V. Coulometric measurements establish that **4** is oxidized by one-electron generating a stable neutral complex $[Fe(L)_2(t\text{-}Bu\text{-}py)]$ ($\mathbf{4^{ox}}$). Chemically **4** can be oxidized yielding the same product by one equivalent of tris(4-bromophenyl)-aminium hexachloroantimonate in CH_3CN at −30 °C. Figure 3 displays the electronic spectra of **4** and chemically generated $\mathbf{4^{ox}}$. The absence of intense maxima >600 nm in the spectrum of **4** and their presence in that of $\mathbf{4^{ox}}$ (810 nm; $\epsilon = 0.6 \times 10^4$ M^{-1} cm^{-1}) are taken as an indication that $\mathbf{4^{ox}}$ has an electronic structure as in $[Fe^{III}(L)(L^{\bullet})(t\text{-}Bu\text{-}py)]$. Thus, the one-electron oxidation of **4** is ligand centered.

The CVs of **5** and **6** have been reported previously.[13] They closely resemble those of **7** and **8** shown in Figure 4 (Table 2). Sellmann et al.[13] have assigned the first two reduction waves at −0.68 V and −1.42 V as metal-centered Fe(IV/III) and Fe(III/II) couples, respectively. The irreversible peak **6** at −0.10 V was proposed to be due the irreversible oxidation of free PMe_3. The quasi-reversible oxidation peak at 0.30 V had been proposed to be due to the metal centered oxidation of five-coordinate **5** to an Fe(V) containing monocation.[13] We disagree with the above interpretations and propose the redox behavior shown in Scheme 3.

First of all, the equilibrium between **7** and **8** and uncoordinated PMe_3 has been experimentally proven to exist by

(19) Herebian, D.; Ghosh, P.; Chun, H.; Bothe, E.; Weyhermüller, T.; Wieghardt, K. *Eur. J. Inorg. Chem.* **2002**, 1957.

(20) Buchanan, R. M.; Pierpont, C. G. *J. Am. Chem. Soc.* **1980**, *102*, 4951.
(21) (a) Jung, O. S.; Pierpont, C. G. *Inorg. Chem.* **1994**, *33*, 2227. (b) Pierpont, C. G.; Jung, O. S. *Inorg. Chem.* **1995**, *34*, 4281.

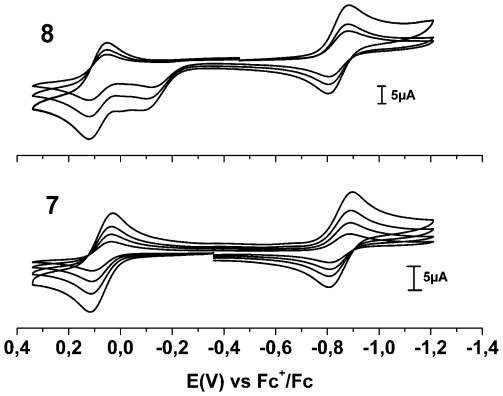

Figure 4. CVs of **7** (bottom) and **8** (top) in CH_2Cl_2 solutions (0.10 M $[N(n\text{-}Bu)_4]PF_6$) at a glassy carbon working electrode at 20 °C. Scan rates: 50, 100, and 200 mV s^{-1} for **7** and 50, 100, 200, and 400 mV s^{-1} for **8**.

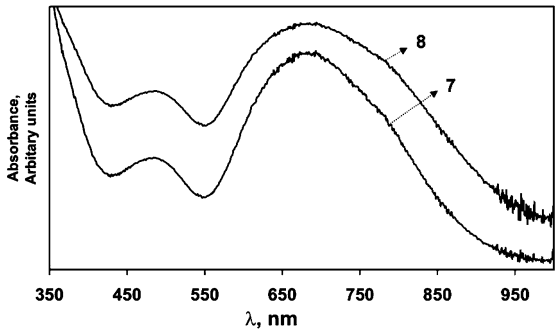

Figure 5. Solid-state electronic spectra of **7** and **8**.

Scheme 3

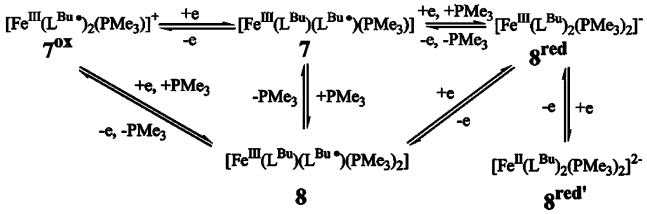

dissolving **8** in CH_3CN and recording the frozen solution Mössbauer spectrum at 80 K (see below). *Two* quadrupole doublets at an approximate ratio of 1:1 representing the spectra of **7** and **8** have been detected. Thus, a solution **8** always contains also **7** and free PMe_3.

The solid-state electronic spectra of **7** and **8** shown in Figure 5 are very similar indeed. Both exhibit a broad band at ~700 nm which is due to the presence of an intervalence charge-transfer band (IVCT) between an $(L^{Bu})^{2-}$ and an $(L^{Bu\bullet})^{1-}$ S,S′-coordinated ligand as in $[Fe^{III}(L^{Bu})(L^{Bu\bullet})(PMe_3)]$ (**7**) and $[Fe^{III}(L^{Bu})(L^{Bu\bullet})(PMe_3)_2]$ (**8**).

Figure 6 shows the spectra of electrochemically generated (−25 °C) $\mathbf{7}^{ox}$ and $\mathbf{8}^{red}$ together with that of a mixture of **7** and **8** in CH_2Cl_2 solution. It is noteworthy that $\mathbf{8}^{red}$, $[Fe^{III}(L^{Bu})_2(PMe_3)_2]^-$, does not show intense absorptions >600 nm which indicates the absence of IVCT bands between $(L^{Bu\bullet})^{1-}$ and $(L^{Bu})^{2-}$. In contrast, the spectrum of $\mathbf{7}^{ox}$ displays two intense maxima at 772 nm ($\epsilon = 1.4 \times 10^4$ M^{-1} cm^{-1}) and 894 nm (0.4×10^4 M^{-1} cm^{-1}) which are due to the presence of two $(L^{Bu\bullet})^{1-}$ ligands as in $[Fe^{III}(L^{Bu\bullet})_2(PMe_3)]^+$.

The electronic spectra of all other complexes have been recorded by using conditions given in Table 3. These spectra are quite revealing. It is important to note that all complexes

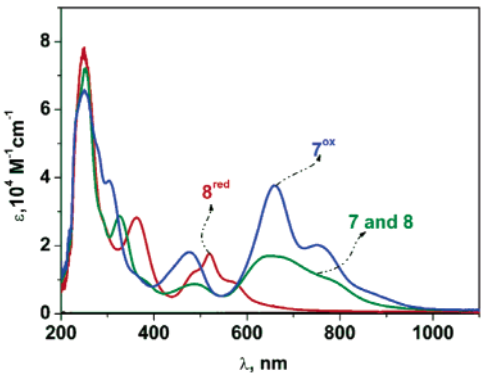

Figure 6. Electronic spectra of a mixture of **7** and **8**, $\mathbf{7}^{ox}$, and $\mathbf{8}^{red}$ in CH_2Cl_2 solution (0.10 M $[N(n\text{-}Bu)_4]PF_6$) at −25 °C.

containing exclusively closed-shell benzene-1,2-dithiolate(2−) ligands (i.e., no ligand radicals) exhibit no absorption maximum >590 nm: this holds for **1**−**4** and $\mathbf{8}^{red}$. It is very important to note that all other complexes exhibit numerous intense (>10^3 M^{-1} cm^{-1}) absorption maxima in the near-infrared between 600 and 1500 nm which cannot be assigned as d−d transitions of an Fe(IV) species. Such bands have been identified as spin- and dipole-allowed ligand-to-ligand charge-transfer bands of the type

$$(L)^{2-}(L^{\bullet})^{1-} \xrightarrow{h\nu} (L^{\bullet})^{1-}(L)^{2-}$$

They are markers for the presence of radical anions $(L^{Bu\bullet})^{1-}$ or $(L^{\bullet})^{1-}$. The energy dependence of this transition (see Table 3) observed in five-coordinate $\mathbf{3}^{ox}$, $\mathbf{4}^{ox}$, **5,** and **7** on the nature of the fifth apical ligand X may be due to the fact that the central iron ion is located slightly but to a varying degree-above the S_4-plane of the two dithiolate ligands.

Infrared Spectra. In a recent publication,[15] we had shown that the presence of S,S′-coordinated radical monoanions, $(L^{Bu\bullet})^{1-}$, is readily detected in the infrared spectrum where the $\nu(C{=}S^{\bullet})$ stretching frequency is observed at ~1100 cm^{-1} as an intense band. In contrast, in complexes containing only the S,S′-coordinated closed-shell dianion $(L^{Bu})^{2-}$ this band is not detected. For example, the spectra of $[N(n\text{-}Bu)_4][Co^{III}(L^{Bu})_2]$ or of the corresponding Au^{III} complex $[N(n\text{-}Bu)_2][Au^{III}(L^{Bu})_2]$ do not show a $\nu(C{=}S^{\bullet})$ band[12] at 1100 cm^{-1}. In contrast, in $[N(n\text{-}Bu)_4][Ni^{II}(L^{Bu})(L^{Bu\bullet})]$ an intense band at 1114 cm^{-1} has been observed.[12]

The spectra of **1**−**4** do not exhibit a $\nu(C{=}S^{\bullet})$ stretching mode at 1100 cm^{-1} in the infrared. Therefore, we conclude that in these compounds only closed-shell $(L^{Bu})^{2-}$ dianions are present. As shown in Figure 7 the species $\mathbf{3}^{ox}$ does display such a band at 1107 cm^{-1} which is again absent in the spectrum of **3**. This is considered to be compelling evidence that the one-electron oxidation of **3** to $\mathbf{3}^{ox}$ is ligand based. Similarly, the infrared spectrum of **7** displays a $\nu(C{=}S^{\bullet})$ band at 1111 cm^{-1} as does the spectrum of **8** at 1117 cm^{-1}. In contrast, the spectrum of $\mathbf{8}^{red}$ of which we had isolated the tetra-*n*-butylammonium salt $[N(n\text{-}Bu)_4][Fe^{III}(L^{Bu})_2(PMe_3)_2]$ lacks this band as is shown in Figure 8. Therefore, it appears to be justified to assign an electronic structure for **7** as $[Fe(L^{Bu})(L^{Bu\bullet})(PMe_3)]$ and for **8** as $[Fe^{III}(L^{Bu})(L^{Bu\bullet})(PMe_3)_2]$.

Sellmann et al.[13] had pointed out that in the infrared spectra of **5** and **6** containing unsubstituted $(L)^{2-}$ ligands no $\nu(C{=}S^{\bullet})$ bands are observed. In fact, this observation had been used to

Table 3. Electronic Spectra of Complexes

complex	conditions[c]	*T*, °C	λ_{max}, nm (ϵ, 10^4 M^{-1} cm^{-1})
1	a	20	315 (0.5), 389 (0.15)
3	b	20	365 (4.15), 590 (3.0), 680 (sh,0.42)
		−60	363 (3.2), 480 (1.4), 530 (1.8), 590 (1.2), 630 (1.1)
$\mathbf{3^{ox}}$ [a]	b	−25	367 (2.7), 495 (1.51), 590 (1.9), 645 (1.8), 860 (0.8)
4	c	20	391 (2.2), 485 (sh,1.5), 512 (1.7)
$\mathbf{4^{ox}}$	c	20	302 (1.6), 360 (1.45), 490 (0.8), 589 (0.9), 670 (0.6), 814 (0.7)
5	d	20	315 (sh,1.6), 360 (sh,0.74), 480 (0.51), 580 (sh,0.48), 645 (0.86), 730 (sh,0.52), 1210 (0.7), 1510(0.8)
7/8[b]	b	−25	320 (2.9), 490 (1.01), 690 (2.0), 789 (0.7), 890 (0.2)
$\mathbf{7^{ox}}$ [a]	b	−25	310 (4.0), 460 (1.9), 692 (4.0), 772 (1.4), 894 (0.4)
$\mathbf{8^{red}}$ [a]	b	−25	360 (2.9), 480 (1.2), 510 (1.9), 570 (1.0)

[a] Electrochemically generated (0.10 M $[N(n\text{-}Bu)_4]PF_6$). [b] Equilibrium mixture. [c] Conditions: (a) tetrahydrofuran solution; (b) CH_2Cl_2 solution; (c) CH_2Cl_2 solution with a few drops of 4-*tert*-butylpyridine; (d) acetone solution (ref 13).

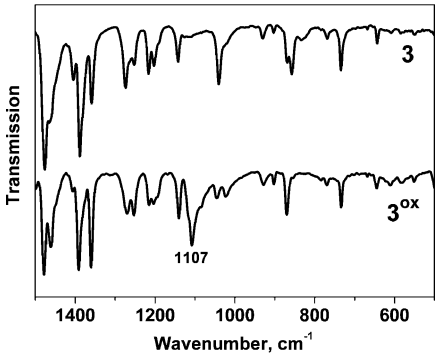

Figure 7. Infrared spectra (KBr disks) of solid **3** (top) and $\mathbf{3^{ox}}$ (bottom) in the range 500−1500 cm^{-1}.

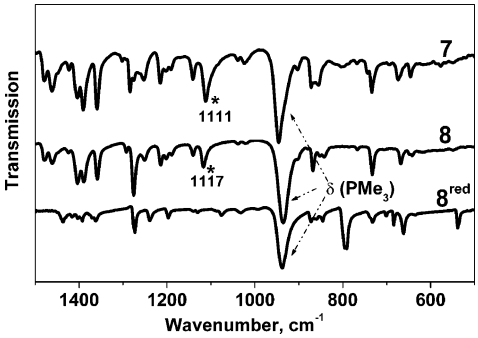

Figure 8. Infrared spectra (KBr disks) of solid **7** (top), **8** (middle), and $[N(n\text{-}Bu)_4][Fe^{III}(L^{Bu})_2(PMe_3)]$, $\mathbf{8^{red}}$ (bottom). The marked bands indicate $\nu(C{=}S^{\bullet})$ frequencies.

propose the presence of only $(L)^{2-}$ ligands and, consequently, iron(IV) metal centers in **5** and **6**. We have verified their observation: **5** and **6** do not display $\nu(C{=}S^{\bullet})$ bands with appreciable intensity but they are nevertheless present in the infrared spectra of **5** and **6** at 1084 cm^{-1}, respectively, as very weak bands. We note that in $[N(CH_3)_4][Fe^{III}(L)_2(PMe_3)_2]$ this band is not observed. From DFT calculations[22] of the vibrational spectra of such complexes which will be reported elsewhere we are able to show that complexes containing 3,5-di-*tert*-butyl-1,2-benzenedithiolate(1−) radicals do exhibit the $\nu(C{=}S^{\bullet})$ band with significant intensity whereas the same vibration is less intense by at least a factor of ∼10 in the corresponding complexes with unsubstituted $(L^{\bullet})^{1-}$ ligands.

Magnetic Properties. All complexes have been investigated by measuring their molar magnetic susceptibilities in the temperature range 2−300 K and 1 T applied field by using a SQUID magnetometer. The magnetic properties of **1** have been

(22) Neese, F. Unpublished work.

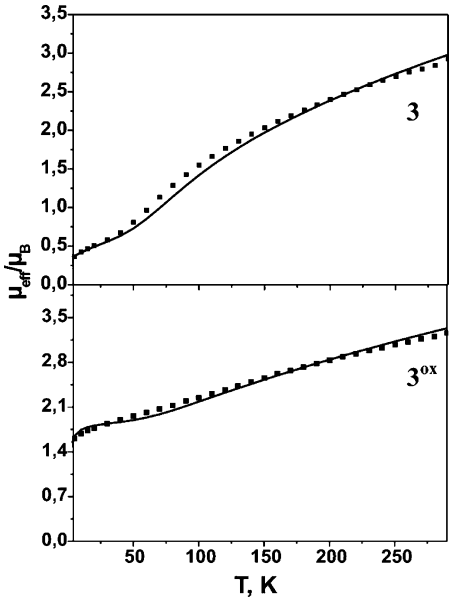

Figure 9. Temperature dependencies of the magnetic moments of solid samples of **3** (top) and $\mathbf{3^{ox}}$ (bottom). The solid lines represent best fits by using parameters given in the text.

reported:[12] $S = 1$; $D = +28$ cm^{-1}; $g_{iso} = 2.05$; $E/D = 0.08$. Thus, **1** contains an intermediate spin ferrous ion.

Figure 9 (top) shows the temperature dependence of the effective magnetic moment of **3** as a function of the temperature. A monotonic decrease of μ_{eff} from 3.0 μ_B at 300 K to 0.4 μ_B at 2 K is indicative of an $S = 0$ ground state and an intramolecular antiferromagnetic coupling between two intermediate spin ferric ions ($S_{Fe} = {}^3/_2$). The best fit of data was achieved with a coupling constant J of -84 cm^{-1} ($H = -2J\ S_1{\cdot}S_2$; $S_1 = S_2 = {}^3/_2$), a fixed $g = 2.0$, and a zero-field splitting parameter $D_1 = D_2 = 15$ cm^{-1}, $E/D = 0$ (fixed) and a paramagnetic impurity with $S = {}^5/_2$ of 1.1%, and a temperature independent paramagnetism χ_{TIP} of 150×10^{-6} emu. The magnetism of **2** (not shown) is very similar: $J = -114$ cm^{-1} ($S_1 = S_2 = {}^3/_2$). $D_1 = D_2 = 5$ cm^{-1}; $E/D = 0$; $g = 2.0$ (fixed); paramagnetic impurity with $S = {}^5/_2$ of 0.6%. It is noted that a reasonable fit of the data can also be obtained assuming the presence of two low spin ferric ions ($S = {}^1/_2$) but this is physically unlikely to be the case because of the fact that monomeric **4** possesses an $S = {}^3/_2$ ground state. It is also not in agreement with its Mössbauer data (see below).

The temperature dependence of the magnetic moments of $\mathbf{3^{ox}}$ shown in Figure 9 (bottom) clearly establishes the $S = {}^1/_2$ ground state of the monoanion (μ_{eff} (4.2 K) = 1.6 μ_B). The increase of

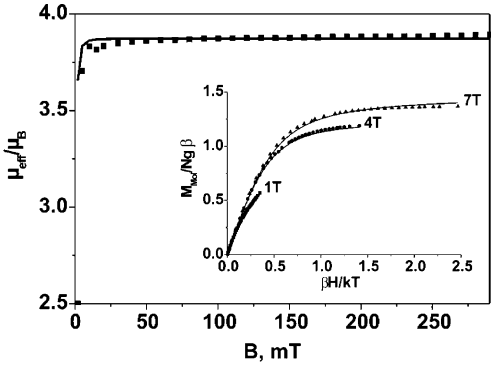

Figure 10. Temperature dependence of the magnetic moment of **4**. The inset shows the magnetization data at 1, 4, and 7 T. For fit parameters see text.

μ_{eff} with increasing temperature was modeled by using a three-spin system $S_1 = S_3 = {}^3/_2$ for the two ferric ions and $S_2 = {}^1/_2$ for the ligand radical $(L^{Bu\bullet})^{1-}$. The following parameters afford the fit shown as solid line in Figure 9: $J_{12} = J_{23} = -28$ cm^{-1}; $J_{13} = -98$ cm^{-1}; $g_1 = g_2 = g_3 = 2.0$ (fixed); $D_1 = D_3 = 15$ cm^{-1}; $E/D = 0$ (fixed), a paramagnetic impurity with $S = {}^5/_2$ of 1.4%, and a TIP of 500×10^{-6} emu. For the data <30 K a small Weiss constant θ of -1.5 K improved the fit. We cannot ascertain if this model is physically meaningful.

The μ_{eff} vs T plot for **4** is shown in Figure 10 together with variable-field, variable-temperature (VHVT) magnetization measurements. The magnetic moment is constant at $3.8\mu_B$ in the range 20−290 K indicating the exclusive population of the spin quartet ground state. Below 20 K μ_{eff} decreases due to magnetization saturation by the applied field of 1 T and the influence of zero-field splitting. The sign of D was determined from VHVT measurements (inset Figure 10). With E/D fixed at 0.32 (from EPR measurements; see below) the magnetization behavior was satisfactorily fitted with $D = -2.3$ cm^{-1} which is in excellent agreement with the analysis of the applied field Mössbauer data of **4**.

For complexes **5** and **6** magnetic moments of $2.75\mu_B$ at 295 K, respectively, have been determined in $CDCl_3$ solution by using Evan's method; for both species an $S = 1$ ground state has been proposed.[13] A more complete analysis for the corresponding complexes **7** and **8** has been performed here where magnetic moments in the range 2−300 K have been measured. Both compounds exhibit temperature-independent magnetic moments in the range 50−300 K of $2.83\mu_B$ typical for $S = 1$ ground states. Below 50 K, the temperature dependence was satisfactorily modeled for **8** by a zero-field splitting parameter $D = +13$ cm^{-1} and a TIP of 375×10^{-6} emu. For **7**, a similar behavior was observed: $D = -27$ cm^{-1}, TIP $= 858 \times 10^{-6}$ emu, and a small Weiss constant θ of 3 K.

EPR Spectroscopy. From magnetic susceptibility data on a solid sample of $\mathbf{3^{ox}}$ it had been established that this species possesses an $S = {}^1/_2$ ground state.[8] As shown in Figure 11 (top), this is confirmed by X-band EPR spectroscopy. An axial signal with $g_x = g_y = 2.06$, and $g_z = 2.01$ ($g_{iso} = 2.04$) has been observed at 10 K in frozen CH_2Cl_2 solution. This spectrum is quite typical for an S-centered radical;[15] it is not in accord with a half-filled d orbital at one of the iron centers. A similar but rhombic signal has been reported for $[Au^{III}(L^{Bu})(L^{Bu\bullet})]$ ($g_x = 2.0690$, $g_y = 2.0320$; $g_z = 1.911$; $g_{iso} = 2.004$).[15]

Compound **4** possesses an $S = {}^3/_2$ ground state; its X-band EPR spectrum is shown in Figure 11 (bottom). It displays a

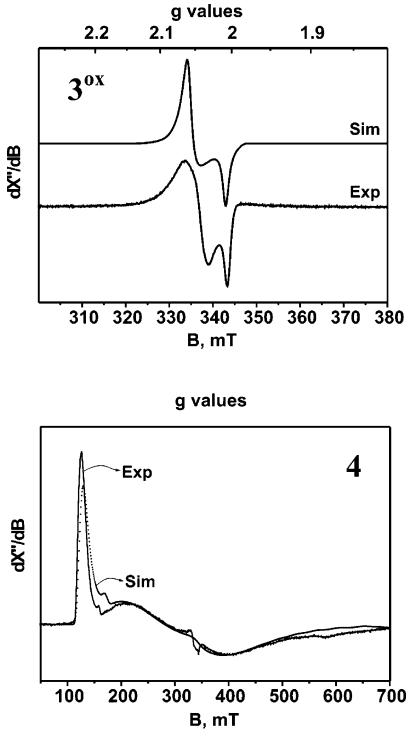

Figure 11. X-band EPR spectra. Top: spectrum of $\mathbf{3^{ox}}$ in CH_2Cl_2 at 10 K (frequency 9.64 GHz; modulation 10.0 G; power 317 μW). Bottom: spectrum of **4** in CH_2Cl_2 at 10 K (frequency: 9.64 GHz; modulation 10.0 G; power 317 μW). For simulation parameters see text.

prominent peak $g = 5-6$ and a broad feature centered at $g \sim 2$. This is indicative of a spin-quartet with a large rhombic zero-field splitting. The spectrum was fitted for $S = {}^3/_2$ by using an axial ZFS parameter $D = 2.2$ cm^{-1} and a rhombicity factor $E/D = 0.32$ which were obtained from the magnetization measurements. Simulations showed that the experimental line width cannot be reproduced with a single set of ZFS parameters. Satisfactory fits were obtained with a Gaussian distribution of E/D values, for which the half-width of the distribution is 0.11. These fit parameters are quite similar to other intermediate spin ferric complexes.[23]

Figure 12 exhibits the X-band EPR spectra at 10 K of $\mathbf{7^{ox}}$ (top) and $\mathbf{8^{red}}$ (bottom) in frozen CH_2Cl_2 both of which possess an $S = {}^1/_2$ ground state. Interestingly, both $\mathbf{7^{ox}}$ and $\mathbf{8^{red}}$ display ^{31}P hyperfine splitting. Satisfactory simulations were obtained by using the following parameters: for $\mathbf{7^{ox}}$: $g_x = 2.18$, $g_y = 2.07$, $g_z = 2.03$; $S = {}^1/_2$; $A_{xx}(^{31}P) = 1.44 \times 10^{-4}$ cm^{-1}, $A_{yy}(^{31}P) = 28.7 \times 10^{-4}$ cm^{-1}, $A_{zz}(^{31}P) = 22.04 \times 10^{-4}$ cm^{-1}; $\mathbf{8^{red}}$: $g_x = 2.15$, $g_y = 2.05$, $g_z = 2.00$; $S = {}^1/_2$; hyperfine coupling to *two* phosphorus nuclei: $A_{xx}(^{31}P) = 6.0 \times 10^{-4}$ cm^{-1}, $A_{yy}(^{31}P) = 33.3 \times 10^{-4}$ cm^{-1}, $A_{zz}(^{31}P) = 35.0 \times 10^{-4}$ cm^{-1}. Note that Sellmann's EPR spectrum of ($[Fe(L)_2(PMe_3)_2]^-$, $S = {}^1/_2$) which is the equivalent of our $\mathbf{8^{red}}$ did not show ^{31}P hyperfine splitting.[13]

Crystal Structures. The crystal structures of **2**, $\mathbf{3^{ox}}$, **4**, **6**, and **9** have been determined or redetermined (**6**). Crystallographic details are given in Table 1. Table 4 summarizes important bond distances. The structure of $[N(n\text{-}Bu)_4]_2[Fe^{III}{}_2(L)_4]$ (**2**) has been determined using a data set collected at 100 K. The room-temperature structure of the tetraethylammonium

(23) (a) Hauser, C.; Bill, E.; Holm, R. H. *Inorg. Chem.* **2002**, *41*, 1615. (b) Hans, M.; Buckel, W.; Bill, E. *Eur. J. Biochem.* **2000**, *267*, 7082.

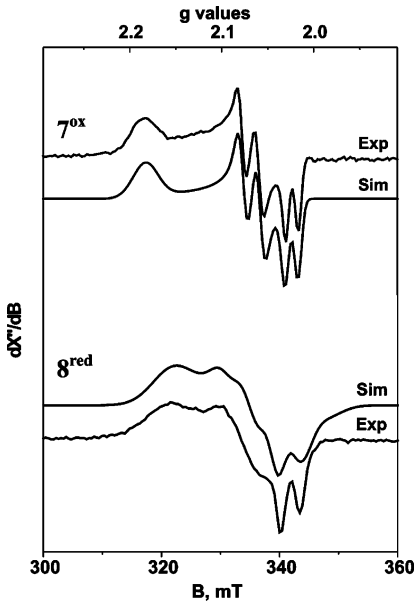

Figure 12. X-band EPR spectra. Top: spectrum of electrochemically generated $\mathbf{7}^{ox}$ in CH_2Cl_2 at 10 K (frequency 9.64 GHz; modulation 10 G; power 323 μW). Bottom: spectrum of $\mathbf{8}^{red}$ in CH_2Cl_2 at 10 K (frequency 9.63; modulation 10 G; power 329 μW). Simulation parameters are given in the text.

salt has been reported previously.[5,6] Complex **2** crystallizes in the triclinic space group $P\bar{1}$ with two crystallographically independent dinuclear dianions $[Fe_2(L)_4]^{2-}$ in the unit cell; each dianion is located on a crystallographic center of symmetry. The two independent dianions adopt different conformations in the solid state. Figure 13 (top) shows one of these; a schematic overlay of the two conformers is shown below. Each five-coordinate iron ion is in a square pyramidal FeS_5 sulfur environment. The two ligands in each $Fe(L)_2$ unit can then either adopt a chair or boat conformation. This is a packing effect because only the $[N(n\text{-}Bu)_4]^+$ salt shows this effect. The average C−S bond length of the nonbridging thiolates at 1.760 ± 0.006 Å is long and indicates the presence of closed-shell benzene-1,2-dithiolates(2−) which in turn requires for the iron ions an oxidation state of +III. Therefore, the electronic structure of **2** is best described as $[Fe^{III}_2(L)_4]^{2-}$.

The structure of the monoanion in crystals of $\mathbf{3}^{ox}$ is very similar to that of the dianion in **2**. Again, two crystallographically independent monoanions are present in the unit cell but in the same conformation as shown in Figure 14. The quality of this crystal structure determination is rather low and does not permit the assignment of the ligand oxidation level(s) or of the metal centers but the atom connectivity is established.

Crystals of **4** consist of well-separated mononuclear anions $[Fe^{III}(L)_2(t\text{-}Bu\text{-}py)]^-$ and $[PMePh_3]^+$ cations (1:1 shown in Figure 15 (top). The average C−S bond length of 1.763 ± 0.006 Å is long and indicates the presence of two S,S′-coordinated, closed-shell ligands $(L)^{2-}$. A neutral 4-*tert*-butylpyridine is located in the apical position of a square pyramidal FeS_4N-polyhedron with a central ferric ion.

The redetermination[13] of the structure of **6** at 100 K has indeed lowered the estimated standard deviations considerably. Figure 15 (middle) shows the structure. The neutral complex possesses a severely distorted octahedral polyhedron comprised of two S,S′-coordinated benzene-1,2-dithiolate ligands and two trimethyl phosphines in *trans*-position relative to each other.

Table 4. Selected Bond Distances (Å)

		Complex **2**	
Fe1−S11	2.2245(6)	S1−C1	1.764(2)
Fe1−S12	2.2305(6)	S2−C2	1.764(2)
Fe1−S1	2.2315(6)	S11−C11	1.750(2)
Fe1−S2	2.2348(6)	S12−C12	1.759(2)
Fe1−S1*	2.4237(6)	S21−C21	1.763(2)
Fe2−S22	2.2225(6)	S22−C22	1.761(2)
Fe2−S31	2.2290(6)	S31−C31	1.758(2)
Fe2−S21	2.2345(6)	S32−C32	1.769(2)
Fe2−S32	2.2367(6)	Fe1−Fe1*	
Fe2−S32*	2.4942(6)	Fe2−Fe2*	
		avg C−C: 1.393 ± 0.01 Å	
		Complex $\mathbf{3}^{ox}$	
Fe1−S4	2.191(4)	S1−C1	1.766(12)
Fe1−S3	2.197(4)	S2−C2	1.778(12)
Fe1−S2	2.215(4)	S3−C21	1.767(13)
Fe1−S1	2.216(4)	S4−C22	1.720(13)
Fe1−S2*	2.327(4)	S5−C41	1.763(12)
Fe2−S8	2.184(4)	S6−C42	1.771(14)
Fe2−S7	2.202(4)	S7−C61	1.712(13)
Fe2−S6	2.209(4)	S8−C62	1.730(11)
Fe2−S5	2.220(4)	Fe1−Fe1*	2.921(4)
Fe2−S6*	2.338(4)	Fe2−Fe2*	2.851(4)
		Complex **4**	
Fe1−N20	2.155(1)	S1−C1	1.755(2)
Fe1−S1	2.2264(4)	S2−C2	1.771(2)
Fe1−S12	2.2336(5)	S11−C11	1.765(2)
Fe1−S11	2.2354(4)	S12−C12	1.760(2)
Fe1−S2	2.2526(5)		
		Complex **6**	
Fe−S11	2.1867(3)	S1−C1	1.750(1)
Fe1−S2	2.1887(3)	S2−C2	1.748(1)
Fe1−S1	2.2894(3)	S11−C11	1.747(1)
Fe1−S12	2.2986(3)	S12−C12	1.749(1)
Fe1−P20	2.3214(3)		
		P20−Fe1−P30	159.79(1)
Fe1−P30	2.3228(3)		
C11−C12	1.407(2)	C1−C2	1.402(2)
C12−C13	1.402(2)	C1−C6	1.405(2)
C13−C14	1.388(2)	C2−C3	1.398(2)
C14−C15	1.395(2)	C3−C4	1.386(2)
C15−C16	1.386(2)	C4−C5	1.396(2)
C16−C11	1.399(2)	C5−C6	1.385(2)
		Complex **9**	
Fe1−S21	2.167(3)	C1−C1	1.768(8)
Fe1−S22	2.190(2)	S2−C2	1.749(8)
Fe1−S1	2.198(2)	S21−C21	1.751(8)
Fe1−S2	2.205(3)	S22−C22	1.765(8)
Fe1−P40	2.284(4)		

For our purpose it is important to note that both thiolato ligands have a somewhat shorter average C−S bond distance at 1.748 ± 0.003 Å than is observed in complexes **2** and **4**. This may be interpreted as ligand oxidation; a dianion $(L)^{2-}$ and a monoanionic radical $(L^{\bullet})^{1-}$ may yield such average C−S distance. All other features are the same as discussed previously by Sellmann et al.[13]

Figure 15 (bottom) shows the structure of the neutral complex $[Fe^{III}(L^{Bu})(L^{Bu\bullet})(PPr_3)]$ in crystals of **9**. In this five-coordinate species the central iron ion is in a square-based pyramidal environment of two S,S′-coordinated thiolato derivatives and an axial phosphine ligand. The structure is very similar to that reported for **5**.[13] The quality of the crystals was not excellent and, therefore, the error of the bond distances is rather large and the average C−S bond length at 1.758 + 0.02 Å does not allow to discern between the presence of two $(L^{Bu})^{2-}$ or one $(L^{Bu})^{2-}$ and one $(L^{Bu\bullet})^{1-}$. The atom connectivity is established beyond doubt. It is interesting that the room-temperature crystal structure of neutral $[Fe(L)_2(PMe_3)]$ displays a short average C−S bond distance at 1.75 Å[13] which may indicate the presence of one $(L)^{2-}$ and one $(L^{\bullet})^{1-}$ ligand. This is also bolstered by the

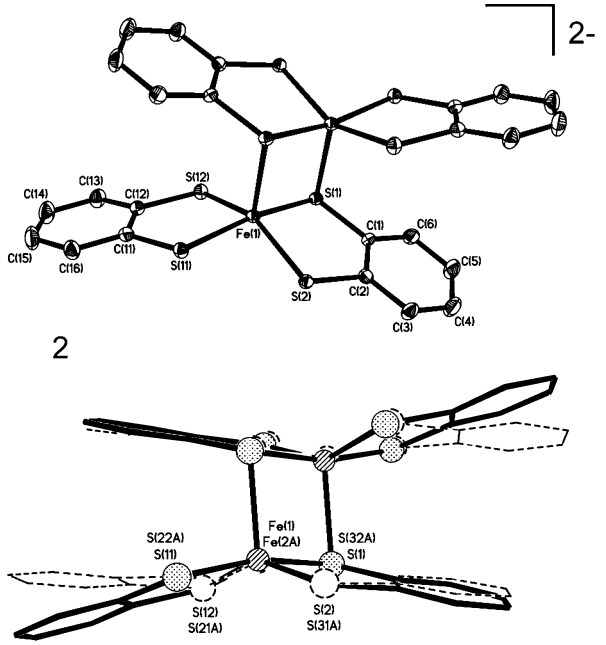

Figure 13. Structure of one of the two crystallographycally independent dianions $[Fe_2(L)_4]^{2-}$ in crystals of **2** (top) and schematic overlay of the two conformers (bottom).

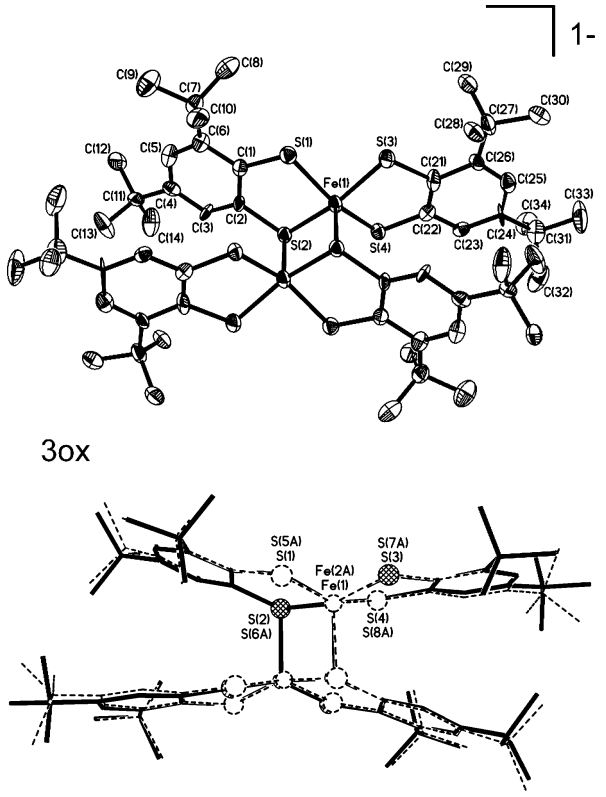

Figure 14. Structure of one of the two crystallographically independent monoanions $[Fe_2(L^{Bu})_4]^-$ (**3ox**) and schematic overlay of both conformers.

observation that both phenyl rings display a weak quinoidal distortion (which is not significant within the 3σ experimental error limit). Thus, the electronic structures of **5** and **9** are probably to be described as $[Fe^{III}(L)(L^{\bullet})(PMe_3)]$ and $[Fe(L^{Bu})(L^{Bu\bullet})(PPr_3)]$, respectively.

We point out that the structures of **6** and **9** both display two equivalent dithiolato ligands; they fail to show structural

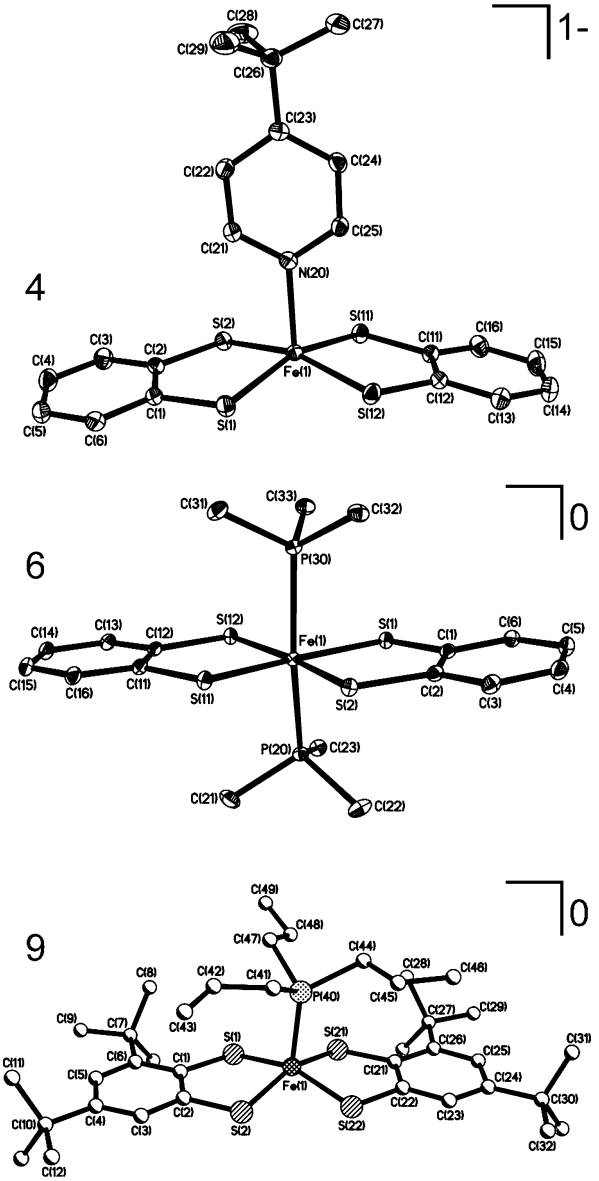

Figure 15. Structure of the monoanions $[Fe^{III}(L)_2(t\text{-Bu-py})]^-$ in crystals of **4** (top), and of the neutral complex $[Fe(L)_2(PMe_3)_2]$ in crystals of **6** and of the neutral species in crystals of **9**.

differences indicative of a localized difference in charge but both do display frequencies at $\sim$1100 cm^{-1} in the infrared indicating the presence of at least one $(L^{Bu\bullet})^{1-}$ radical. We will show in a subsequent paper that the square planar complexes $[M(L^{Bu})(L^{Bu\bullet})]^-$ ($M = Ni^{II}$, Pd^{II}, Pt^{II}) also exhibit this band. From density functional calculations it is deduced that the ligand mixed valency between $(L^{Bu})^{2-}$ and $(L^{Bu\bullet})^{1-}$ is of delocalized class III. Thus we propose that in complexes **7** and **8** a similar behavior may be expected.

Mössbauer Spectroscopy. Complexes **1**−**9** have been carefully investigated by applied-field (1−7 T) Mössbauer spectroscopy at 4.2 K and detailed spin Hamiltonian analyses have been carried out. In addition, zero-field Mössbauer spectra of polycrystalline or frozen solution samples were recorded at 80 K. The results are summarized in Tables 5 and 6.

The spectra of the square planar intermediate spin ferrous species $[NH(C_2H_5)_3]_2[Fe^{II}(L)_2]$ ($S = 1$) have been reported and discussed previously.[11,12] The following spin Hamiltonian parameters were found at 4.2 K: $S = 1$, zero-field splitting

Table 5. Zero-Field Mössbauer Data of Complexes

complex	δ,[a] mm s^{-1}	ΔE_Q,[b] mm s^{-1}	Γ,[c] mm s^{-1}	T, K	S_{Fe}[d]	S_t[e]	ref
1	0.44	1.20	0.28	80	1	1	11, 12
	0.45	1.21	0.28	4.2			
2	0.31	2.95	n.m.[f]	77	1.5	0	6
3	0.36	2.87	0.44	80	1.5	0	this work
3^{ox}	0.28	2.70	0.46	80	1.5	0.5	this work
4	0.33	3.03	0.31	80	1.5	1.5	this work
4^{ox}	0.29	3.02	0.29	80	1.5	1.0	this work
5	0.12	3.03	0.31	4.2	1.5	1.0	13
6	0.17	1.54	0.29	86	1.5	1.0	13
6^{red}	0.29	1.67	0.38/0.32	92	0.5	0.5	13
7	0.11	3.18	0.28	80	1.5	1.0	this work
7^{ox}	0.25	2.60	0.36	80	1.5	0.5	this work
8	0.15	1.46	0.29	80	1.5	1.0	this work
8^{red}	0.24	1.56	0.28	80	0.5	0.5	this work
9	0.09	3.19	0.30	80	1.5	1.0	this work

[a] Isomer shift. [b] Quadrupole splitting. [c] Half width of signal. [d] Intrinsic spin ground state of iron ion. [e] Spin ground state of molecule. [f] Not measured.

$D = +28$ cm^{-1}, $E/D = 0.08$; isomer shift $\delta = 0.45$ mm s^{-1}, quadrupole splitting $\Delta E_Q = +1.21$ cm^{-1}, asymmetry parameter $\eta = 0.44$; nuclear hyperfine coupling constants $A_{xx}/g_N\beta_N = -4.15$ T, $A_{yy}/g_N\beta_N = -5.58$ T, and $A_{zz}/g_N\beta_N = +0.18$ T. We will use these data as benchmark for an intermediate spin ferrous ion.[24]

Similarly, the data for the five-coordinate anion $[Fe^{III}(L)_2(t\text{-Bu-py})]^-$ in **4** may serve as benchmark values for an intermediate spin ferric ion ($S_{Fe} = {}^3/_2$);[25−29] see Tables 5 and 6. The Mössbauer spectra were recorded on frozen CH_3CN solutions of **4** in order to minimize possible intermolecular magnetic interactions. Figure 16 displays the spectra and their simulations at 0.1, 1, 4, and 7 T. These values are reassuringly similar to those reported for other five-coordinate, intermediate spin ferric complexes[25−28] (Table 6). Hallmarks are a quite large quadrupole splitting of >3.0 mm s^{-1} as well as two major negative components and a minor positive one of the **A** tensor. This anisotropy is, in general, attributed to the spin dipolar term. Since the latter is traceless, the contact contribution can be obtained by averaging the principal components of **A**. The value $A_{Fe}/g_N\beta_N$ of −16.6 T compares also well with other five-coordinate intermediate spin ferric complexes.[25−29] The nature of the donor atoms (sulfur or nitrogen) does not appear to play a dominant role. These data give us confidence to assign an intermediate spin ferric electronic structure in complexes by applied-field Mössbauer spectroscopy.

For example, the diamagnetic dinuclear complexes **2** and **3** exhibit each a single quadrupole doublet with isomer shift and quadrupole splitting parameters which are nearly identical to those of **4** (Table 5). Therefore, we feel confident to assign local spin states of ${}^3/_2$ to each of two ferric ions in both dinuclear

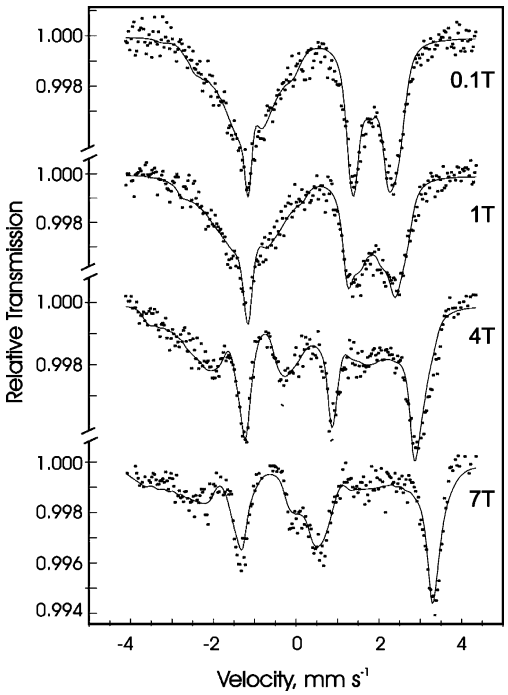

Figure 16. Applied field Mössbauer spectra of **4** in frozen CH_3CN solution at 4.2 K and 0.1, 1, 4, 7 T fields. For fit parameters see Table 6.

complexes where the intramolecular antiferromagnetic spin coupling does not allow an independent direct determination of the individual ${}^3/_2$ spin states by magnetic measurements. We also note that the reported Mössbauer parameters for $[N(n\text{-Bu})_4]_2[Fe^{III}_2(dcbdt)_4]$[8] ($dcbdt^{2-}$ = 4,5-dicyanobenzene-1,2-dithiolate(2−)), namely $\delta = 0.32$ mm s^{-1}; $\Delta E_Q = 3.01$ mm s^{-1} at 75 K, are again identical to those mentioned above. In our view this rules out an interpretation as low-spin ferric ($S_{Fe} = {}^1/_2$) as was proposed by the authors.[7]

Up to this point, the oxidation states of the iron ions and their spin ground states are unequivocally determined by magnetic susceptibility measurements, X-ray crystallography, and Mössbauer spectroscopy. They are in all cases fairly straightforwardly determined because the thiolato ligands are always redox-innocent, i.e., they are S,S′-coordinated closed-shell dianions. This is not so for the one-electron oxidized form of **3**, namely the dinuclear monoanion with $S = {}^1/_2$ in crystals of **3^{ox}**. Simple charge considerations immediately imply that in case of a metal-centered one-electron oxidation a mixed valent $Fe^{III}-Fe^{IV}$ monoanionic species with four benzene-1,2-dithiolato(2−) ligands is generated or, alternatively, if a ligand-centered oxidation prevails, an $[Fe^{III}_2(L^{Bu})_3(L^{Bu\bullet})]^-$ species is formed with two intermediate spin ferric ions and three $(L^{Bu})^{2-}$ ligands plus one radical $(L^{Bu\bullet})^{1-}$. The zero-field Mössbauer spectrum of **3^{ox}** displays a *single* quadrupole doublet which rules out the mixed valent $Fe^{III}Fe^{IV}$ formulation. The isomer shift and quadrupole splitting parameters for **3^{ox}** are in excellent agreement with those of **2**, **3**, and **4** indicating the presence of two intermediate spin ferric ions. Thus the oxidation of **3** to **3^{ox}** is ligand-centered.

Interestingly, one-electron oxidation of mononuclear **4** yielding neutral **4^{ox}** is also *not* accompanied by significant changes of the isomer shift or quadrupole splitting parameters (Table 5). Thus, a frozen CH_3CN solution at 80 K of **4** to which 1 equivalent of the oxidant tris(4-bromophenyl)aminium hexachlo-

(24) (a) Barraclough, C. G.; Martin, R. L.; Mitra, S.; Sherwood, R. C. *J. Chem. Phys.* **1970**, *53*, 1643. (b) Hudson, A.; Whitefield, H. J. *Inorg. Chem.* **1967**, *6*, 1120. (c) Moss, T. H.; Robinson, A. B. *Inorg. Chem.* **1968**, *7*, 1692.
(25) Niarchos, D.; Kostikas, A.; Simopoulos, A.; Coucouvanis, D.; Piltingsrud, D.; Coffman, R. E. *J. Chem. Phys.* **1978**, *69*, 4411.
(26) Kostka, K. L.; Fox, B. G.; Hendrich, M. P.; Collins, T. J.; Rickard, C. E.; Wright, L. J.; Münck, E. *J. Am. Chem. Soc.* **1993**, *115*, 6746.
(27) Keutel, H.; Käpplinger, I.; Jäger, E.-G.; Grodzicki, M.; Schünemann, V.; Trautwein, A. X. *Inorg. Chem.* **1999**, *38*, 2320.
(28) Koch, W. O.; Schünemann, V.; Gerdan, M.; Trautwein, A. X.; Krüger, H.-J. *Chem. Eur. J.* **1998**, *4*, 686.
(29) (a) Gupta, G. P.; Lang, G.; Scheidt, W. R.; Geiger, D. K.; Reed, C. A. *J. Chem. Phys.* **1986**, *85*, 5212. (b) Gupta, G. P.; Lang, G.; Reed, C. A.; Shelly, K.; Scheidt, W. R.; Geiger, D. K. *J. Chem. Phys.* **1987**, *86*, 5288.

roantimonate had been added at −30 °C shows a single quadrupole doublet: $\delta = 0.29$ mm s^{-1}, $\Delta E_Q = 3.02$ mm s^{-1} for **4^{ox}**. This indicates again a ligand-centered oxidation and the electronic structure of **4^{ox}** is best described as [Fe^{III}(L^{Bu})-(L$^{Bu•}$)(*t*-Bu-py)] S = 1 with an intermediate spin ferric ion ($S_{Fe} = {}^3/_2$) coupled antiferromagnetically to a ligand radical (L$^{Bu•}$)$^{1-}$.

The square-based pyramidal complex **5**[13] is isoelectronic with **4^{ox}**; only the axial trimethylphosphine in **5** is substituted by a 4-*tert*-butylpyridine ligand in **4^{ox}**. It is therefore not surprising that both compounds have similar zero-field Mössbauer parameters. The quadrupole splitting is 3.03 mm s^{-1} for **5** and 3.02 mm s^{-1} for **4^{ox}** at 80 K; the isomer shifts differ slightly by $\Delta\delta = 0.17$ mm s^{-1} where δ is 0.29 mm s^{-1} for **4^{ox}** and 0.12 mm s^{-1} for **5**. Such a shift of δ has previously been shown to also occur in isoelectronic [Fe^{II}(pyS$_4$)X] complexes[30] where X is either a bridging thiolate ($\delta = 0.44$ mm s^{-1}) or a trimethylphosphine ($\delta = 0.34$ mm s^{-1}). The Mössbauer parameters for five-coordinate **9** are also very similar to those of **5** and **4^{ox}**. Thus, all of these species possess an intermediate spin central ferric ion ($S = {}^3/_2$) and one (L^{Bu})$^{2-}$ or (L)$^{2-}$ as well as one radical monoanion (L$^{Bu•}$)$^{1-}$ or (L$^{•}$)$^{1-}$ affording the observed $S = 1$ ground states: [Fe^{III}(L)(L$^{•}$)(PMe$_3$)] (**5**), [Fe^{III}(L)(L$^{•}$)(t-Bu-py)] (**4^{ox}**), and[Fe^{III}(L^{Bu})(L$^{Bu•}$)(PPr$_3$)] (**9**). Complex **7** is also isoelectronic and "isostructural" with **5** and the Mössbauer parameters are again nearly identical (Tables 5 and 6). The electronic structure of **7** is therefore [Fe^{III}(L^{Bu})(L$^{Bu•}$)(PMe$_3$)] with a central intermediate spin ferric ion coupled antiferromagnetically to a ligand radical (L$^{Bu•}$)$^{1-}$ affording the observed $S = 1$ ground state. The zero-field Mössbauer spectrum of the frozen CH$_3$-CN solution of the one-electron oxidized form **7^{ox}** ($S = {}^1/_2$) displays also a single quadrupole doublet ($\delta = 0.25$ mm s^{-1}; $\Delta E_Q = +2.60$ mm s^{-1}). These parameters again indicate the presence of an intermediate spin ferric ion but now two ligand radicals must be present yielding the observed $S = {}^1/_2$ ground state: [Fe^{III}(L$^{Bu•}$)$_2$(PMe$_3$)]$^+$. The alternative description[13] as Fe^V species, namely [Fe^V(L^{Bu})$_2$(PMe$_3$)]$^+$, is not at all compatible with the spectroscopic data presented here. In this case it is again observed that one-electron oxidation of [Fe^{III}(L^{Bu})(L$^{Bu•}$)-(PMe$_3$)] (**7**) with $S = 1$ ground-state yielding [Fe^{III}(L$^{Bu•}$)$_2$-(PMe$_3$)]$^+$ with $S = {}^1/_2$ is a ligand-centered process; both species contain a central intermediate spin ferric ion.

The applied field Mössbauer spectra of distorted octahedral **8** are shown in Figure 17; the results of the spin Hamiltonian analysis are given in Table 6. The parameters are very similar to those reported for all intermediate spin ferric complexes with the exception of a smaller quadrupole splitting parameter of only +1.46 mm s^{-1} as compared to an average value of 3.0 mm s^{-1} for the five-coordinate intermediate spin complexes **4**, **7**, and **7^{ox}**. Interestingly, Krüger et al.[28] have recently reported a similar, octahedral ferric complex [Fe^{III}(L-N$_4$Me$_2$)(S$_2$C$_6$H$_4$)]-(ClO$_4$)·0.5H$_2$O ($S_{Fe} = {}^3/_2$; $\delta = 0.38$ mm s^{-1}, $\Delta E_Q = 2.22$ mm s^{-1} at 200 K) which also exists in a low spin ferric form ($S_{Fe} = {}^1/_2$; $\delta = 0.25$ mm s^{-1}, $\Delta E_Q = 2.22$ mm s^{-1} at 200 K). The latter Mössbauer parameters agree nicely with those measured for **8^{red}** in Table 5. Thus, the electronic structures are best descibed as intermediate spin ferric ($S_{Fe} = {}^3/_2$) in **8** and low spin ferric in **8^{red}**: [Fe^{III}(L$^{Bu•}$)(L^{Bu})(PMe$_3$)$_2$] ($S = 1$) and [Fe^{III}(L^{Bu})$_2$(PMe$_3$)$_2$]$^-$ ($S = {}^1/_2$), respectively. Complex **8** cannot be described as Fe(IV) species. The Mössbauer data for Sellmann's[13] complex [NMe$_4$][Fe^{III}(L)$_2$(PMe$_3$)$_2$]·CH$_3$OH ($\delta = 0.29$ mm s^{-1}; $\Delta E_Q = 1.67$ mm s^{-1} at 92 K) are in excellent agreement with our frozen solution data for **8^{red}**.

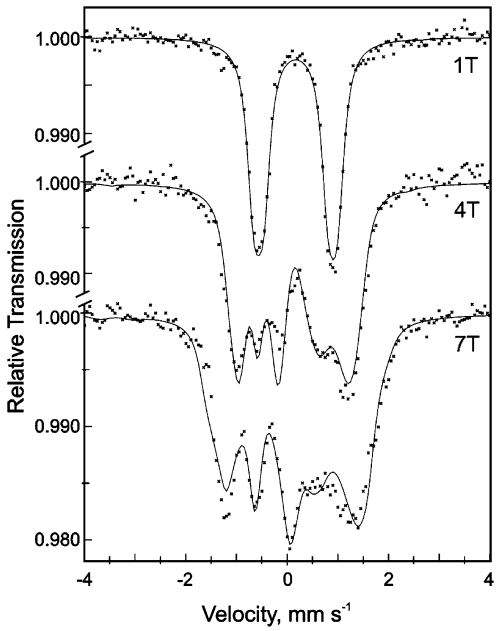

Figure 17. Applied field Mössbauer spectra of **8** at 4.2 K and 1, 4, 7 T fields. For fit parameters see Table 6.

Discussion

The most important goal of the present investigation is to establish unequivocally the electronic structure of some five-coordinate iron complexes containing two S,S′-coordinated benzene-1,2-dithiolato type ligands and a fifth (axial) phosphine ligand, [Fe(L)$_2$(PR$_3$)], in a square-base pyramidal FeS$_4$P donor atom set. The problem rests entirely on the ability to identify spectroscopically a square planar [Fe^{III}(L)(L$^{•}$)]^0 vs an [Fe^{IV}(L)$_2$]^0 moiety. In other words, the question is whether benzene-1,2-dithiolates behave here as redox-noninnocent ligands with the sulfur analogues of a catecholate or benzosemiquinonate radical being present in a given coordination compound.

Many authors[7,13] have attempted to discern between a dithiolato(2-) and its monoanionic radical form in a given complex by their crystallographically determined structural parameters. The underlying assumption has always been that the phenyl ring has either six equidistant C−C bonds in a thiolate or displays a quinoidal distortion with two alternating shorter C═C bonds and four longer ones in the radical form and, in addition, the C−S bonds were assumed to shrink upon oxidation of a dianionic thiolate to a monoanionic radical. This behavior had been firmly established for the corresponding complexes containing catecholates and semiquinonates.[31] This is—in part—a misconception for the sulfur analogues. The structures of the phenoxyl and the thiyl radical have been calculated by theoretical computational methods.[32,33] The results clearly show that the expected structural changes in comparison

(30) Li, M.; Bonnet, D.; Bill, E.; Neese, F.; Weyhermüller, T.; Blum, N.; Sellmann, D.; Wieghardt, K. *Inorg. Chem.* **2002**, *41*, 3444.

(31) Pierpont, C. G.; Lange, C. W. *Progr. Inorg. Chem.* **1994**, *33*, 331.
(32) (a) Qin, Y.; Wheeler, R. A. *J. Am. Chem. Soc.* **1995**, *117*, 6083. (b) Himo, F.; Gräslund, A.; Erikson, L. A. *Biophys. J.* **1997**, *72*, 1556. (c) Adamo, R.; Subra, A.; Di Matteo, A.; Barone, V. *J. Chem. Phys.* **1998**, *109*, 10244.
(33) Tripathi, G. N. R.; Sun, Q.; Armstrong, D. A.; Chipman, D. M.; Schuler, R. H. *J. Phys. Chem.* **1992**, *96*, 5344.

Table 6. Applied Field Mössbauer Parameters of Intermediate Spin Ferric Complexes at 4.2 K

complex	S_t	δ (mm s^{-1})	ΔE_Q (mm s^{-1})	$A_{xx}/g_N\beta_N$ (T)	$A_{yy}/g_N\beta_N$ (T)	$A_{zz}/g_N\beta_N$ (T)	$\langle A\rangle/g_N\beta_N$ (T)	$A_{Fe}{}^d/g_N\beta_N$ (T)	D (cm^{-1})	E/D	$D_{Fe}{}^e$ (cm^{-1})	h
3^{ox}	0.5	0.27	2.67	+2.5	−25.1	−28.6	−17.1					0.3
4[a]	1.5	0.34	2.94	−19.13	−32.24	1.54	−16.61	−16.61	−3.80	0.33	−3.80	0.02
7	1.0	0.12	3.05	−32.43	−22.16	0.35	−18.08	−14.46[f]	−28.0	0.01	−18[h]	0.74
7^{ox}	0.5	0.29	2.57	−31.10	−32.74	1.68	−20.72	−8.31[g]				0.45
8	1.0	0.17	1.46	1.56	−12.35	−38.22	−16.34	−13.07[f]	14.35	0.01	9.0[h]	0.10
L′FeCl[b]	1.5	0.25	3.60	−22	−16.6	5	−11.8	−11.8	−3.70	0.05	−3.7	0.15
LFeI[c]	1.5	0.19	3.56	−12.7	−12.7	0.5	−8.3	−8.3	13	0.22	13	0.0

[a] Frozen acetonitrile solution. [b] See ref 26. [c] See ref 27. [d] Intrinsic A component for $S_{Fe} = {}^3/_2$. [e] Intrinsic D value for $S_{Fe} = {}^3/_2$. [f] $A_{Fe} = {}^4/_5\langle A\rangle$. [g] $A_{Fe} = {}^2/_5\langle A\rangle$. [h] $D_{Fe} = {}^2/_3D$.

Table 7. Compilation of Intrinsic Mössbauer Parameters for Five-Coordinate Complexes in Figure 18

complex	S_t[a]	S_{Fe}[b]	δ[c] (mm s^{-1})	ΔE_Q[d] (mm s^{-1})	$\mathbf{A}(S_{Fe} = {}^3/_2)/g_N\beta_N$[e] (T)	ref
$[Fe^{III}(L)_2(t\text{-}Bu\text{-}py)]^{1-}$	$^3/_2$	$^3/_2$	0.34	+2.94	−19.1, −32.2, +1.54	this work
$[Fe^{III}(L_O{}^{ISQ\bullet})_2I]$	$^1/_2$	$^3/_2$	0.24	+2.80	−12.4, −20.3, +1.3	36
$[Fe^{III}(L_S{}^{ISQ})_2I]$	$^1/_2$	$^3/_2$	0.12	3.18	−7.4, −16.0, +0.6	36
$[Fe^{III}(L^{Bu})(L^{Bu\bullet})(PMe_3)]^0$	1	$^3/_2$	0.12	+3.05	−25.9, −17.7, +0.3	this work
$[Fe^{III}(L^{Bu\bullet})_2(PMe_3)]^+$	$^1/_2$	$^3/_2$	0.29	+2.57	−12.44, −13.1, +0.68	this work
$[Fe^{III}(L)I]$	$^3/_2$	$^3/_2$	0.19	3.56	−12.7, −12.7, +0.5	27
$[Fe^{III}(L')Cl]$	$^3/_2$	$^3/_2$	0.25	3.60	−22, −16.6, +5	26

[a] Ground state of molecule. [b] Intrinsic ground state of iron ion. [c] Isomer shift at 4.2 K relative to α-Fe at 298 K. [d] Quadrupole splitting at 4.2 K. [e] $\mathbf{A}(S_{Fe} = {}^3/_2)$: tensor components from spin projection techniques where appropriate.

with their closed-shell phenolate and thiophenolate forms are only observed for the phenoxyl but not the thiyl. This observation is due to the fact that the spin density distribution of both radicals differ. In a phenoxyl only 38% of the spin density resides on the oxygen atom, 24% is found at each of the two ortho carbon atoms and 32% is at the para carbon. In contrast, in the thiyl radical 68% of the spin density resides at the sulfur atom and only 32% is delocalized over the ortho and para positions of the phenyl ring. Consequently, the six C−C distances in a thiyl radical resemble more closely those of the aromatic thiolate analogue but the C−S bond is slightly shorter at 1.75 Å. Therefore, structural parameters may be of only limited value for the identification of a benzene-1,2-dithiolate-(1−) radical in a given complex. On the other hand, in the series $[Ni^{II}(L^{Bu})_2]^{2-/1-/0}$ the neutral species $[Ni^{II}(L^{Bu\bullet})_2]^0$ contains two $(L^{Bu\bullet})^{1-}$ radicals and here the structural parameters are distinctly different from those of the dianion $[Ni^{II}(L^{Bu})_2]^{2-}$.[34]

As pointed out by us previously[15] in complexes containing the radical anion $(L^{Bu\bullet})^{1-}$, the ν(C═S•) stretching frequency is clearly observed as a relatively intense band in the infrared at 1100 cm^{-1}. This band is absent in the corresponding complexes containing only $(L^{Bu})^{2-}$ ligands. This is in accord with a resonance Raman study of the phenylthiyl radical for which the predominantly ν(C═S•) mode has been observed at 1073 cm^{-1} (ν_{7a} Wilson mode).[33] We propose that this band is a significant spectroscopic marker for the presence of an S,S′-coordinated $(L^{Bu\bullet})^{1-}$ radical. As noted above, the present complexes **3^{ox}**, **7**, and **8** display such a band.

Sellmann et al.[13] had pointed out that in the infrared spectra of **5** and **6** containing unsubstituted $(L)^{2-}$ ligands no ν(C═S•) bands are observed. In fact, this observation had been used to propose the presence of only $(L)^{2-}$ ligands and, consequently, iron(IV) metal centers in **5** and **6**. We have verified their observation: **5** and **6** do not display ν(C═S•) bands with appreciable intensity but they are nevertheless present in the infrared spectra of **5** and **6** at 1084 cm^{-1}, respectively, as very weak bands. We note that in $[N(CH_3)_4][Fe^{III}(L)_2(PMe_3)_2]$ this band is not observed. From DFT calculations[22] of the vibrational spectra of such complexes which will be reported elsewhere we are able to show that complexes containing 3,5-di-*tert*-butyl-1,2-benzenedithiolate(1−) radicals do exhibit the ν(C═S•) band with significant intensity whereas the same vibration is less intense by at least a factor of ∼10 in the corresponding complexes with unsubstituted $(L^{\bullet})^{1-}$ ligands.

The second important spectroscopic marker for the presence of an $M(L^{Bu})(L^{Bu\bullet})$ and/or $M(L)(L^{\bullet})$ moiety is the observation of an intense (∼10^4 M^{-1} cm^{-1}) intervalence transition $M(L)(L^{\bullet}) \leftrightarrow M(L^{\bullet})(L)$ in the near-infrared. These intense bands with intensities >0.5 × 10^4 M^{-1}cm^{-1} cannot be assigned as transitions from the π-orbital levels of the isolated radical ligands. Complex $[(bpy)Pt^{II}(L^{Bu\bullet})]^+$ displays such an intraligand π-π^* transition[14] at 700 nm but with an absorption coefficient of only 1.0 × 10^3 M^{-1}cm^{-1}. A similar ligand-to-ligand band is observed for all square planar complexes $[M(L^{\bullet})_2]^n$.[35] Thus, this band has been reported for $[Au^{III}(L^{Bu})(L^{Bu\bullet})]^0$ at 1452 nm (ϵ = 2.7 × 10^4 M^{-1} cm^{-1})[15] and for $[Ni^{II}(L^{Bu})(L^{Bu\bullet})]^-$ at 860 nm (ϵ = 1.2 × 10^4 M^{-1} cm^{-1}).[34] These bands are absent in their one-electron reduced forms $[Au^{III}(L^{Bu})_2]^-$ and $[Ni^{II}(L^{Bu})_2]^{2-}$. In the present series of iron complexes we noted that all complexes containing exclusively two $(L^{Bu})^{2-}$ or $(L)^{2-}$ ligands do not display absorption maxima of intensities >500 M^{-1} cm^{-1} above 600 nm (complexes **1**, **2**, **3**, **4**, **6^{red}**, and **8^{red}**). Their respective electronic structure should therefore be described as shown in Scheme 1 with dianionic aromatic ligands. In contrast, complexes **3^{ox}** (860 nm (0.8 × 10^4 M^{-1} cm^{-1})), **4^{ox}** (814 nm (0.7 × 10^4 M^{-1} cm^{-1})), **5** (1210 nm (0.7 × 10^4), 1510 nm (0.8 × 10^4 M^{-1} cm^{-1})),[13] **7/8** (890 nm (0.2 × 10^4 M^{-1} cm^{-1})), display this absorption and, therefore, are proposed to contain a $[Fe^{III}(L^{Bu})(L^{Bu\bullet})]$ or a $[Fe^{III}(L)(L^{\bullet})]$ moiety. The presence of $[Fe^{IV}$-

(34) Sellmann, D.; Binder, H.; Häussinger, D.; Heinemann, F. W.; Sutter, J. *Inorg. Chim. Acta* **2000**, *300*−*302*, 829.

(35) (a) Herebian, D.; Bothe, E.; Neese, F.; Weyhermüller, T.; Wieghardt, K. *J. Am. Chem. Soc.* **2003**, *125*, 9116. (b) Herebian, D.; Wieghardt, K.; Neese, F. *J. Am. Chem. Soc.* **2003**, *125*, 10997.

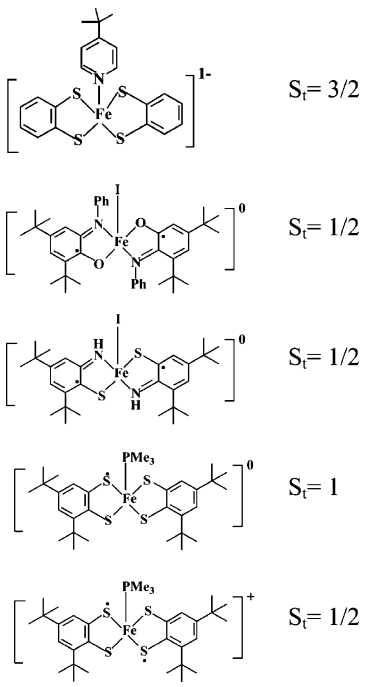

Figure 18. Five-coordinate complexes containing none, one, and two π radical ligands and a central intermediate spin ferric ion ($S_{Fe} = {}^3/_2$) yielding $S_t = {}^3/_2$, $S_t = 1$, and $S_t = {}^1/_2$ ground states, respectively.

$(L)_2]$ is ruled out. Complex **7**^{ox} is proposed to be $[Fe^{III}(L^{Bu\bullet})_2(PMe_3)]^+$ with two $(L^{Bu\bullet})^{1-}$ radical ligands (894 nm (0.4×10^4 M^{-1} cm^{-1}).

The third very valuable marker for a correct assignment of the electronic structure of these complexes is zero- and applied-field ^{57}Fe Mössbauer spectroscopy. The spectra for mononuclear **4** ($S_t = {}^3/_2$) represent the benchmark for a pure intermediate spin ferric ion in a square base pyramidal ligand environment (Tables 5,6). When the measured **A**-tensor components A_{ii} of **7** ($S = 1$), **7**^{ox} ($S = {}^1/_2$), and **8** ($S = 1$) in Table 6 are converted to intrinsic values for $S_{Fe} = {}^3/_2$ by using spin-projection techniques, one obtains the intrinsic $\mathbf{A}(S_{Fe} = {}^3/_2)/g_N\beta_N$ values in Table 6. The values obtained agree nicely with those reported for well-characterized five-coordinate intermediate-spin ferric complexes with redox-innocent ligands (Table 7). In particular, the similarity of the pronounced **A** anisotropies with the unusual positive **z** component is significant. Furthermore, large quadrupole splittings at $\sim$3 mm s^{-1} and a positive electric field gradient (EFG) component V_{zz} along the minor component of the **A**-tensor were recognized as additional characteristic features of intermediate-spin iron(III). We have previously reported detailed analyses of the Mössbauer spectra of complexes $[Fe^{III}(L^{\bullet}_{rad})_2X]$ where $(L^{\bullet}_{rad})^{1-}$ represents an *o*-iminobenzosemiquinonate or its thio analogue (Figure 18 and Table 7).[36] From these spectroscopic data (Tables 6 and 7) it is evident that complexes **5**−**9** contain an intermediate spin ferric ion and one antiferromagnetically coupled ligand radical $(L^{\bullet})^{1-}$ or $(L^{Bu\bullet})^{1-}$. It is not possible to interpret the Mössbauer data in Tables 5 and 6 consistently by assuming the presence of high valent iron(IV) ions.

Acknowledgment. We thank Dr. Ameerunisha Begum for the synthesis and characterization of **2**. We are grateful to the Fonds der Chemischen Industrie for financial support, and K.R. thanks the Max-Planck Society for a stipend.

Supporting Information Available: X-ray crystallographic tables for complexes. This material is available free of charge via the Internet at http://pubs.acs.org.

JA040237L

(36) Ghosh, P.; Bill, E.; Weyhermüller, T.; Wieghardt, K. *J. Am. Chem. Soc.* **2003**, *125*, 3967.